

Superradiant scattering of electromagnetic fields from ringing black holes

Rajesh Karmakar^{1,*} and Debaprasad Maity^{1,†}

¹*Department of Physics, Indian Institute of Technology Guwahati, Assam 781039, India*

Detection of gravitational waves (GWs) paves the beginning of a new era of gravitational wave astronomy. Black holes (BHs) in their ringdown phase provide the cleanest signal of emitted GWs that imprint the fundamental nature of BHs under low energy perturbation. Apart from GWs, any complementary signature of ringing BHs can be of paramount importance. Motivated by this we analyzed the scattering of electromagnetic waves in such a background and demonstrated that the absorption cross section of a ringing Schwarzschild BH can be superradiant. Moreover, we have found out that such superradiant phenomena are transient in nature with a characteristic time scale equal to the GW oscillation time scale. We further point out that the existing ground-based Low Frequency Array (LOFAR), radio telescopes, may be able to detect such transient signals from BHs of mass range $M \sim 10^{-1} - 10^{-2} M_{\odot}$, which should necessarily be of primordial origin. Our present result opens up an intriguing possibility of observing the black hole merging phenomena through electromagnetic waves.

I. INTRODUCTION

The past few years have been very exciting in the field of gravity after the detection of GWs by LIGO, VIRGO, and KAGRA[1–15] which significantly enhanced our understanding the nature of gravity and BHs in particular. The merging of binary BHs is a remarkable cosmic event, and the detection enables us for the first time to see those hidden phenomena through their gravitational wave emission. The whole merging process of two BHs usually consists of three distinct phases, inspiral, merging and ringdown (for binary BH observations see [1, 9], for numerical simulations, one may look at [16–19]). In our present submission, we particularly focus on analysing characteristic features of a BH in its ringdown phase (which we shall refer as ringing BH) when interacting with external fields. In the previous study [20], to the best of our knowledge, we for the first time investigated the scattering of an ultralight scalar field with a ringing Schwarzschild BH and demonstrated that the field may experience superradiant scattering, particularly in the infrared regime. However, the detection of such transient superradiant signals in the scalar sector is experimentally challenging. In this paper, we investigate instead the scattering of electromagnetic (EM) fields which is experimentally more relevant. Apart from direct gravitational waves, any complementary signature such as time dependent superradiance scattering of EM waves from ringing BH could be of paramount importance in light of the recent spate of research activity on the aspects of black holes, and gravitational waves in particular.

EM waves interacting with a gravitational wave have been explored in the literature[21–23]. Phenomena of superradiance have been the subject of investigation for quite some time, for scalar waves [24], for EM waves [25–29], particularly from rotating BHs. The possibility of

moving BHs [30] causing superradiant amplification has also been explored in the literature. On the observational front, the dynamics of fundamental fields in time dependent background have been the subject of investigation in recent times[31], where the superradiant evolution leads to significant enhancement in the emitted flux. The dynamical character of the superradiance very often gives rise to interesting effects in BH shadow[32, 33] and polarization [34, 35]. In this paper, we initiate a novel study of electromagnetic wave scattering through the ringing black hole background.

The rest of the paper is organized in the following manner. First, we briefly describe the ringing black hole space time (details can be found in [20, 36]). Then we derive the governing equation to study the dynamics of the EM field in this background. We build up the framework to calculate the absorption cross-section fixing boundary conditions of the EM field accordingly. We then define the absorption cross section with approximate normalization suitable for the oscillating BH. Finally, we present our numerical results with subsequent discussion on the possible observational scenarios and conclusion.

We will use the metric signature as $(-, +, +, +)$ and follow the natural units, $\hbar = c = G = 1$, throughout the discussion.

II. RINGING BLACK HOLE BACKGROUND

The end stage of the binary BH merger, the well known ringdown phase, can be theoretically modelled by applying perturbation theory on a static BH spacetime. For our present purpose the static part of the ringing BH is assumed to be Schwarzschild. In the perturbative limit the ringing BH can be mathematically expressed in the following manner, $g_{\mu\nu} = g_{\mu\nu}^s + h_{\mu\nu}$, where $g_{\mu\nu}^s$ is the standard Schwarzschild metric. $h_{\mu\nu}$ is the gravitational wave (GW) perturbation. We further consider the quadrupole oscillation with orbital angular mode $l_0 = 2$, azimuthal angular mode $m_0 = 0$ (note that quasinormal mode frequency does not depend on m_0 [37]), of the GW

* rajesh018@iitg.ac.in

† debu@iitg.ac.in

part. This oscillating (ringing) part (see Appendix. A of [20] for details) is expressed in radiation gauge [36], which captures the correct asymptotic behaviour of the GW flux as,

$$h_{\mu\nu} = \frac{1}{2}e^{-i\omega t} \times \begin{pmatrix} Hf(r)Y_2^0 & H_1Y_2^0 & 0 & 0 \\ H_1Y_2^0 & Hf(r)^{-1}Y_2^0 & h_1^{(e)}\partial_\theta Y_2^0 & h_1^{(o)}s_\theta\partial_\theta Y_2^0 \\ 0 & h_1^{(e)}\partial_\theta Y_2^0 & r^2\mathcal{T}_2^0 & \frac{1}{2}h_2\mathcal{I}_2^0 \\ 0 & h_1^{(o)}s_\theta\partial_\theta Y_2^0 & \frac{1}{2}h_2\mathcal{I}_2^0 & r^2s_\theta^2\mathcal{T}_2^0 \end{pmatrix} + h.c. \quad (1)$$

where, symbols are, $\mathcal{I}_2^0 = (c_\theta\partial_\theta Y_2^0 - s_\theta\partial_\theta^2 Y_2^0)$, $\mathcal{T}_2^0 = KY_2^0 + G\partial_\theta^2 Y_2^0$, and $\tilde{\mathcal{T}}_2^0 = KY_2^0 + \cot\theta G\partial_\theta Y_2^0$. $s_\theta = \sin\theta$, $c_\theta = \cos\theta$ and Y_l^m is the spherical harmonics. The time dependent part of the ringing fluctuation is expressed as $e^{-i\omega t}$, with ω being quasi-normal frequency. The perturbation variables are divided into parity odd ($h_1^{(o)}, h_2$) and parity even ($h_1^{(e)}, H, H_1, K, G$) radial coordinate (r) dependent functions. Einstein's equation governing the ringing perturbation variables boils down to the well known Regge-Wheeler equations[37–39]

$$\frac{d^2\tilde{Z}_i}{dr_*^2} + (\omega^2 - V_i)\tilde{Z}_i = 0, \quad (2)$$

where, $i \equiv (\mathcal{E}, \mathcal{O})$ are associated with \mathcal{E} ven and \mathcal{O} dd perturbation. $r_* = r + 2M \ln(r/2M - 1)$ is the Tortoise coordinate. For quadrupole oscillation, the potentials assume the following form,

$$V_{\mathcal{E}} = f(r) \frac{8(3r^3 + 3Mr^2) + 18M^2(2r + M)}{r^3(2r + 3M)^2},$$

$$V_{\mathcal{O}} = f(r) \left(\frac{6}{r^2} - \frac{6M}{r^3} \right). \quad (3)$$

Where, $f(r) = 1 - 2M/r$ is the Schwarzschild metric function, and M is the mass of the black hole. The functional dependence of odd parity variables $\tilde{Z}_{\mathcal{O}}(r)$ and even parity variables $\tilde{Z}_{\mathcal{E}}(r)$ are explicitly derived in [36, 39]. The near horizon values of the ringing fields will be parameterized by ($|\tilde{Z}_{\mathcal{O}}(r \rightarrow 2M)| = \mathcal{O}_h$, $|\tilde{Z}_{\mathcal{E}}(r \rightarrow 2M)| = \mathcal{E}_h$). By solving the Regge-Wheeler equations with the quasi-normal mode boundary conditions [40, 41]; ingoing near the event horizon and outgoing near spatial infinity one will be able to construct the full solution of ringing Schwarzschild BH background (1). Now, our aim is to solve the minimally coupled EM equation in such a background.

III. MINIMALLY COUPLED GAUGE FIELD

The minimally coupled EM field satisfies the standard equation of motion as,

$$\frac{1}{\sqrt{-g}}\partial_\mu(\sqrt{-g}g^{\mu\alpha}g^{\nu\beta}F_{\alpha\beta}) = 0. \quad (4)$$

Since the non-ringing part of the background is spherically symmetric, we decompose the EM field components as [42]

$$A_t(t, \mathbf{r}) = \sum_{lm} b^{lm}(t, r)Y_{lm}(\Omega),$$

$$A_r(t, \mathbf{r}) = \sum_{lm} h^{lm}(t, r)Y_{lm}(\Omega),$$

$$A_s(t, \mathbf{r}) = \sum_{lm} [k_{lm}(t, r)\Psi_s^{lm}(\Omega) + a_{lmk}(t, r)\Phi_s^{lm}(\Omega)], \quad (5)$$

where we have used the well known orthogonal vector spherical harmonic basis [43, 44] for the azimuthal field components,

$$\Psi_s^{lm} = \partial_s Y_{lm},$$

$$\Phi_s^{lm} = \epsilon_{ss'}\partial^{s'} Y_{lm}. \quad (6)$$

Where, s, s' indices correspond to angular coordinates (θ, ϕ) and $\epsilon_{\theta\theta} = \epsilon_{\phi\phi} = 0$, $\epsilon_{\theta\phi} = -\epsilon_{\phi\theta} = \sin\theta$. In our analysis, we work with the following gauge invariant variables,

$$\chi_1^{lm} = \frac{r^2}{l(l+1)}(\partial_t h^{lm} - \partial_r b^{lm}) ; \quad \chi_2^{lm} = a^{lm}, \quad (7)$$

$$\chi_3^{lm} = h^{lm} - \partial_r k^{lm} ; \quad \chi_4^{lm} = b^{lm} - \partial_t k^{lm}.$$

(see [42] for stationary BHs). The governing dynamical equation of the electromagnetic potentials in terms of gauge invariant variables up to linear order in fluctuations are,

$$\mathcal{L}_s \chi_1^{lm} + \sum_{c\gamma} \mathcal{Q}_{lmc\gamma}^i(h)\chi_i^{c\gamma} + \sum_{c\gamma} \bar{\mathcal{Q}}_{lmc\gamma}^i(h^*)\chi_i^{c\gamma} = 0,$$

$$\mathcal{L}_s \chi_2^{lm} + \sum_{c\gamma} \mathcal{R}_{lmc\gamma}^i(h)\chi_i^{c\gamma} + \sum_{c\gamma} \bar{\mathcal{R}}_{lmc\gamma}^i(h^*)\chi_i^{c\gamma} = 0, \quad (8)$$

with \mathcal{L}_s being a Klein-Gordon operator for static Schwarzschild BH,

$$\mathcal{L}_s = f(r)\partial_r(f(r)\partial_r) - \partial_t^2 - f(r)\frac{l(l+1)}{r^2}, \quad (9)$$

where $i \rightarrow (1, 2, 3, 4)$, and $\mathcal{Q}_{lmc\gamma}^i, \mathcal{R}_{lmc\gamma}^i, \bar{\mathcal{Q}}_{lmc\gamma}^i, \bar{\mathcal{R}}_{lmc\gamma}^i$ (for detailed expression see the appendix A), are the differential operators dependent on the first-order complex and its conjugate part of the metric fluctuation “ h ” respectively. The other two gauge invariant variables turned out to satisfy the following constrained equations,

$$f(r)\partial_r \chi_1^{lm} + \chi_4^{lm} = 0,$$

$$\partial_t \chi_1^{lm} + f(r)\chi_3^{lm} = 0. \quad (10)$$

Utilizing these equations we can calculate χ_3 and χ_4 in terms of the other two gauge invariant variables. We will now follow the perturbative method to obtain the solution and compute the flux to study the absorption cross-section. Working in terms of gauge invariant variables,

we are expecting that it would be possible to avoid the ambiguity of the gauge fixing process in the whole procedure. The ringing background is constructed out of quadrupole perturbation, and hence the spherical symmetry of the system under study is naturally lost. As a consequence, different angular modes of the EM field will be coupled to each other. To decouple the angular part from (8) we proceed via considering perturbative expansion of the field χ^{lm} as,

$$\chi_i^{lm}(t, r) = \chi_{i(b)}^{lm}(t, r) + \chi_{i(p)}^{lm}(t, r) + \dots, \quad (11)$$

where we apply the perturbative expansion counting the order of $h_{\mu\nu}$. "b" denotes the solution for the static background and "p" denotes the perturbed part. Substituting the above expansion in (8) we obtain the linearized equations of motion as,

$$\begin{aligned} \mathcal{L}_s \chi_{1(b)}^{lm} &= 0, \\ \mathcal{L}_s \chi_{1(p)}^{lm} + \sum_{c\gamma} \mathcal{Q}_{lmc\gamma}^i(h) \chi_{i(b)}^{c\gamma} + \sum_{c\gamma} \bar{\mathcal{Q}}_{lmc\gamma}^i(h^*) \chi_{i(b)}^{c\gamma} &= 0. \end{aligned} \quad (12)$$

and

$$\begin{aligned} \mathcal{L}_s \chi_{2(b)}^{lm} &= 0, \\ \mathcal{L}_s \chi_{2(p)}^{lm} + \sum_{c\gamma} \mathcal{R}_{lmc\gamma}^i(h) \chi_{i(b)}^{c\gamma} + \sum_{c\gamma} \bar{\mathcal{R}}_{lmc\gamma}^i(h^*) \chi_{i(b)}^{c\gamma} &= 0. \end{aligned} \quad (13)$$

By using the properties of the inhomogeneous differential equation, we now simplify the above inhomogeneous equations (12)(13), with the decomposition of the fields taken as, $\chi_{1(p)}^{lm} = \chi_{1,p}^{lm} + \bar{\chi}_{1,p}^{lm}$ and $\chi_{2(p)}^{lm} = \chi_{2,p}^{lm} + \bar{\chi}_{2,p}^{lm}$, such that,

$$\mathcal{L}_s \chi_{1,p}^{lm} + \sum_{c\gamma} \mathcal{Q}_{lmc\gamma}^i \chi_{i(b)}^{c\gamma} = 0; \quad \mathcal{L}_s \bar{\chi}_{1,p}^{lm} + \sum_{c\gamma} \bar{\mathcal{Q}}_{lmc\gamma}^i \chi_{i(b)}^{c\gamma} = 0 \quad (14)$$

and

$$\mathcal{L}_s \chi_{2,p}^{lm} + \sum_{c\gamma} \mathcal{R}_{lmc\gamma}^i \chi_{i(b)}^{c\gamma} = 0; \quad \mathcal{L}_s \bar{\chi}_{2,p}^{lm} + \sum_{c\gamma} \bar{\mathcal{R}}_{lmc\gamma}^i \chi_{i(b)}^{c\gamma} = 0. \quad (15)$$

We only consider the particular solution for the $\chi_{1,p}^{lm}$, $\bar{\chi}_{1,p}^{lm}$ and $\chi_{2,p}^{lm}$, $\bar{\chi}_{2,p}^{lm}$. Fixing the initial condition for $\chi_{1,(b)}^{lm}$ and $\chi_{2,(b)}^{lm}$ would be sufficient, as the source term depends (along with the ringing metric components) on the zeroth order solution of the EM field. The above set of equations can be thought of as EM waves propagating in the static Schwarzschild ($g_{\mu\nu}^s$) background with oscillatory source term. Therefore, to solve this we set the following ingoing boundary condition near the horizon of the static BH, with arbitrary normalization constant as, $\mathcal{N}_{1(b)} = \zeta_1^{lm} e^{-ikt} f(r)^{-2iMk}$ and $\mathcal{N}_{2(b)} = \zeta_2^{lm} e^{-ikt} f(r)^{-2iMk}$, for $\chi_{1,(b)}^{lm}$ and $\chi_{2,(b)}^{lm}$ respectively. Similarly, we obtain the zeroth order solutions for $\chi_{3(b)}^{lm}$ and $\chi_{4(b)}^{lm}$ from the coupled equations (10). Once the zeroth order solutions are obtained we substitute these solutions to the inhomogeneous eq. (14) and (15) and again solve the equations numerically.

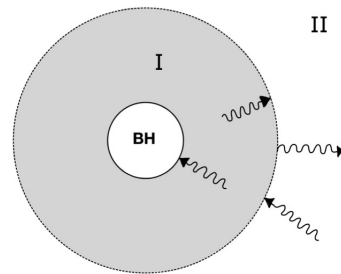


FIG. 1. We demonstrate the inclusion of the hypothetical interaction surface in the ringing black hole space time. Shaded region (I) is considered as the space time containing ringing fluctuations and outside region (II) is considered as the usual Schwarzschild space time.

IV. SETTING UP THE BOUNDARY CONDITION

In the static Schwarzschild space time, asymptotic flatness helps us to normalize the field solution such that an incoming wave of unit amplitude from infinity gets scattered by the BH potential. Such normalization is used to define [45] the absorption cross section of a static BH. For our present case, however, the ringing BH background being oscillatory in nature does not have the same asymptotic structure. Further, due to quadrupole perturbation, spherical symmetry is also lost. Therefore, to compute the absorption cross section for such a case, we proposed a methodology in our earlier paper [20], and for completeness, we outline the important steps here. We introduce a hypothetical surface fig.1 at some radial distance $r = r_{\text{int}}$ from the BH event horizon calling it an *interaction surface*. The wave coming towards the black hole is assumed to perceive the presence of ringing BH once it hits the interaction surface. Outside the surface $r > r_{\text{int}}$, the spacetime is assumed to be approximately static Schwarzschild BH, and this is the approximation which helps us to appropriately define the normalization of the incoming wave. We label the region inside the interaction surface as region-I, and outside as region-II. With this setup, the EM wave solution in region-I will assume,

$$\chi_{\text{I}}^{klm}(t, r) = \chi_{(b)}^{klm} + \chi_{(p)}^{klm} + \bar{\chi}_{(p)}^{klm} + \dots \quad (16)$$

where, $\chi \equiv (\chi_1, \chi_2)$, i.e. the expansion of both χ_1^{klm} and χ_2^{klm} have the same structure, hence we suppress the notation in this section. In the region-II, it would be in the background of static Schwarzschild BH, as

$$\chi_{\text{II}}^{klm}(t, r) = \chi_s^{klm} \quad \text{with} \quad \mathcal{L}_s \chi_s^{klm} = 0. \quad (17)$$

To solve the above second order partial differential equation (the field solution at the interaction surface may not be separable in space and time) in Region-II, the approx-

ropriate boundary condition would be as follows,

$$\begin{aligned}
\chi_{\mathbf{II}}^{klm}(t, r)|_{\forall t, r \rightarrow r_{\text{int}}} &= \chi_{\mathbf{I}}^{klm}(t, r)|_{\forall t, r \rightarrow r_{\text{int}}}, \\
\partial_r \chi_{\mathbf{II}}^{klm}(t, r)|_{\forall t, r \rightarrow r_{\text{int}}} &= \partial_r \chi_{\mathbf{I}}^{klm}(t, r)|_{\forall t, r \rightarrow r_{\text{int}}}, \\
\chi_{\mathbf{II}}^{klm}(t, r)|_{t \rightarrow \infty, \forall r} &= \chi_{\mathbf{b}}^{klm}(t, r)|_{t \rightarrow \infty, \forall r}, \\
\partial_t \chi_{\mathbf{II}}^{klm}(t, r)|_{t \rightarrow \infty, \forall r} &= -ik \chi_{\mathbf{b}}^{klm}(t, r)|_{t \rightarrow \infty, \forall r}.
\end{aligned} \tag{18}$$

The first two boundary conditions arise naturally for the hypothetical interaction surface. Whereas the last two boundary conditions arise due to the following reason: at a fixed distance from the black hole r , ringing oscillation amplitude decays exponentially with time due to its quasinormal nature. Therefore, in $t \rightarrow \infty$ limit, the perturbative components of the gauge field, $(\chi_{(\text{p})}^{klm}, \tilde{\chi}_{(\text{p})}^{klm})$ which are the explicit function of $h_{\mu\nu}$ must also be vanishing at the interaction surface. Such a condition will naturally ensure the calculated absorption cross-section of ringing BH reducing to its static Schwarzschild value within the characteristic time scale of the oscillation $\tau \sim 2\pi/\omega$. By employing the boundary condition described in Eq.18, we proceed to solve Eq.17 in the domain, $([r_{\text{int}}, \infty], [t_{\text{int}}, \infty])$ lying inside light cone, $t \geq r_*$. The asymptotic nature of the GWs is better expressed in the outgoing null coordinates. Therefore, after obtaining the solution, we perform a transformation into the outgoing null coordinate system. $(t, r) \rightarrow (u = t - r_*, r)$ using $\tilde{A}_\mu(x') = (\partial x^\nu / \partial x'^\mu) A_\nu(x)$ [46] and define the absorption cross-section accordingly as described in the following section.

V. DEFINING ABSORPTION CROSS SECTION

We use the following definition of the absorption cross section defined at spacial infinity that encapsulates the stress energy tensor of the EM field,

$$\sigma_{\text{ring}}^{kl}(u, r_{\text{int}}) \equiv \frac{\partial_u \mathcal{F}^{kl}}{\partial_u \mathcal{G}^k}. \tag{19}$$

Where the total energy being absorbed by the ringing BH per unit time is given by,

$$\partial_u \mathcal{F}^{kl} = \int d\Omega r^2 \mathcal{T}^r{}_u. \tag{20}$$

After integrating over the angular variables, the energy absorption rate is expressed in terms of gauge invariant variables as,

$$\begin{aligned}
\partial_u \mathcal{F}^{kl} &= l(l+1) \times \\
&\times \left[\frac{1}{2} \left\{ \tilde{\chi}_3^{klm}(u, r) \tilde{\chi}_4^{klm*}(u, r) + \tilde{\chi}_4^{klm}(u, r) \tilde{\chi}_3^{klm*}(u, r) \right. \right. \\
&+ \partial_r \tilde{\chi}_2^{klm}(u, r) \partial_u \tilde{\chi}_2^{klm*}(u, r) + \partial_u \tilde{\chi}_2^{klm}(u, r) \partial_r \tilde{\chi}_2^{klm*}(u, r) \\
&\left. \left. - \left\{ \tilde{\chi}_4^{klm}(u, r) \tilde{\chi}_4^{klm*}(u, r) + \partial_u \tilde{\chi}_2^{klm}(u, r) \partial_u \tilde{\chi}_2^{klm*}(u, r) \right\} \right].
\end{aligned} \tag{21}$$

Note that to define the absorption cross-section we used ingoing light-cone coordinate (u, r) , in which all the field variables are expressed in ‘‘tilde’’ when transforming from $(t, r) \rightarrow (u, r)$ (see Appendix.D for details derivation).

Now, the incident energy density per unit time for a plane EM wave propagating in the z -direction is constructed as

$$\partial_u \mathcal{G}^k = \mathcal{T}^z{}_u. \tag{22}$$

Having evaluated the solution of the EM wave in spherical coordinates with a damped oscillating time dependent feature we find it convenient to recast the expression for incident energy density in the spherical coordinates as,

$$\begin{aligned}
\partial_u \mathcal{G}^k &= \left\{ \frac{1}{2} g^{ss} (\partial_u A_s - \partial_s A_u) (\partial_r A_s^* - \partial_s A_r^*) + c.c. \right\} \\
&- g^{ss} (\partial_u A_s - \partial_s A_u) (\partial_u A_s^* - \partial_s A_u^*).
\end{aligned} \tag{23}$$

With the help of (5) and (7) one can express (of course one has to take care of the coordinate transformation from (t, r) to (u, r) the following combinations in terms of the invariant variables turns out to be,

$$\begin{aligned}
\partial_u A_s - \partial_s A_u &= \sum_{lm} [(\partial_r \tilde{\chi}_1^{klm} - \partial_u \tilde{\chi}_1^{klm}) \Psi_s^{lm}(\Omega) + \partial_u \tilde{\chi}_2^{klm} \Phi_s^{lm}(\Omega)], \\
\partial_r A_s - \partial_s A_r &= \sum_{lm} [\partial_r \tilde{\chi}_1^{klm} \Psi_s + \partial_r \tilde{\chi}_2^{klm} \Phi_s].
\end{aligned} \tag{24}$$

In case of oscillating BH, individual normalization of $\tilde{\chi}_1^{klm}$ and $\tilde{\chi}_2^{klm}$ can be obtained by assuming an approximate asymptotic form,

$$\begin{aligned}
\tilde{\chi}_1^{klm}(u, r) &= \mathcal{N}_1^{klm} [\mathcal{I}_1(u) e^{-ik(u+2r_*)} + \mathcal{R}_1(u) e^{-iku}], \\
\tilde{\chi}_2^{klm}(u, r) &= \mathcal{N}_2^{klm} [\mathcal{I}_2(u) e^{-ik(u+2r_*)} + \mathcal{R}_2(u) e^{-iku}],
\end{aligned} \tag{25}$$

where the coefficients, $(\mathcal{I}_1(u), \mathcal{R}_1(u))$ and $(\mathcal{I}_2(u), \mathcal{R}_2(u))$ are related to ingoing (incident) and outgoing (reflected) wave amplitude of $\tilde{\chi}_1^{klm}(u, r)$ and $\tilde{\chi}_2^{klm}(u, r)$ respectively. We evaluate these amplitudes numerically from the solutions of $\tilde{\chi}_1^{klm}(u, r)$ and $\tilde{\chi}_2^{klm}(u, r)$. Now comparing the above two expressions with the same quantities constructed (see Appendix.B) for circularly polarized incident plane EM wave we derive the normalization factors as,

$$\begin{aligned}
\mathcal{N}_1^{klm} &= -i(-1)^{l+1} \delta_{m1} \sqrt{\frac{4\pi(2l+1)}{l(l+1)}} \frac{1}{2k\mathcal{I}_1(u \rightarrow \infty)}, \\
\mathcal{N}_2^{klm} &= (-1)^l \delta_{m1} \sqrt{\frac{4\pi(2l+1)}{l(l+1)}} \frac{1}{2k\mathcal{I}_2(u \rightarrow \infty)}.
\end{aligned} \tag{26}$$

Where δ_{m1} appears due to the fact that the EM field potentials, $A_\mu(x)$, transforms as a vector, and that shows up in the spherical wave expansion of the incident plane EM wave with azimuthal index $m = 1$ [29]. We also normalize the combinations of (24) by dividing the right hand

side with $\sum_{lm} (-1)^{l+1} \delta_{m1} \sqrt{\frac{4\pi(2l+1)}{l(l+1)}} [\Phi_s^{lm}(\Omega) + i\Psi_s^{lm}(\Omega)]$, consequently the gauge invariant combinations finally become,

$$\begin{aligned} \partial_u A_s - \partial_s A_u &= \xi_{us}(k, l, u) (-ik A'_s(u, \mathbf{r})), \\ \partial_r A_s - \partial_s A_r &= \xi_{rs}(k, l, u) (-2ik A'_s(u, \mathbf{r})), \end{aligned} \quad (27)$$

with the nontrivial time dependent coefficients, $\xi_{us}(k, l, u)$, $\xi_{rs}(k, l, u)$ with the property that they become unity as the static limit, $u \rightarrow \infty$, of the ringing BH is approached (for details one may look at Appendix.B). Importantly, the sum in (24) with normalization factors exhibits a convergent nature for increasing l having alternative $+/-$ sign in the summation, therefore, we have taken up to $l = 6$ for our numerical analysis. Whereas, $A'_s(u, \mathbf{r})$, denotes the spherical polar expansion [29] of the incident circularly polarized EM wave, which can be suitably factored out from the expression of the incident energy density.

VI. NUMERICAL RESULTS

As previously mentioned, the ringing BH background is constructed taking only the quadrupole oscillation [47] or the lowest $l(= 2)$ mode with the corresponding quasinormal frequency $\omega = (0.74734 - i 0.17792)(r_h)^{-1}$ [41, 48]. $r_h = 2M$ is the horizon radius for the Schwarzschild BH. The chosen frequency is known to be the long-lived one among all the other modes. Further, the frequency for both even and odd parity perturbation was found to be the same as per the existing literature [40, 41, 48]. All physical quantities and associated parameters have been made dimensionless utilizing the characteristic scale, r_h . We consider the solution of the background ringing field for which the perturbative scheme is valid ensuring $\delta g/g_s \propto h_\mu^\mu \ll 1$ for a diverse range of initial parameters. Once the solution for the ringing black hole background is obtained, we solve for the EM field Eq.17. Unless stated throughout our presentation we have shown the results for a fixed background amplitude, $\mathcal{E}_h, \mathcal{O}_h \sim 10^{-5}$ within the perturbative limit. As mentioned earlier, as a consistency check we also reproduce the well studied static limit of the absorption cross-section [26] of Schwarzschild BH for EM field in the limit, $\lim_{u \rightarrow \infty} \sigma_{\text{ring}}^{kl}(u, r_{\text{int}}) = \sigma^s(k, l)$.

We evaluate the absorption cross section at $r \sim 75r_h$ and further numerically ensure that all the necessary results remain intact even afterwards, apart from very small fluctuations induced by numerical precisions due to the extension of the domain of the solutions. Our final results are summarized in Figs.2 and 3.

According to our construction, time dependent boundary conditions at the interaction surface would introduce time varying features in the absorption cross section. Such transient nature of the GWs is clearly seen to be imprinted in the behaviour of EM absorption cross section and exhibits the quasi-periodic oscillation

along with its characteristic time scale. One can indeed observe that within the GW time scale $\tau_{\text{GW}} \sim 35r_h$ associated with the quasinormal frequency $\omega = (0.74734 - i 0.17792)(r_h)^{-1}$, the EM absorption cross-section $\sigma^{kl}(u, r_{\text{int}})$ undergoes a time dependent oscillation, which can assume large negative values, and this negative amplitude of the absorption cross-section precisely signifies the phenomena of superradiant scattering.

We identify five main theory parameters of our interest (k, l, r_{int}) and the GW amplitudes $(\mathcal{E}_h, \mathcal{O}_h)$. However, for all our practical purposes we choose both the GW amplitudes to be the same. With decreasing GW amplitude the EM superradiant amplitude is expected to decrease which we have consistently observed in our numerical results, and indeed be seen in the second panel of the Fig. 2. This also provides us confidence as a consistency check of our numerical methodology. We provide the plots choosing the interaction surface located at $r_{\text{int}} \sim 20r_h$. Interestingly, the superradiant amplitude turned out to be maximum at $r_{\text{int}} \sim 20 - 25r_h$ for all angular modes, l and frequency, k that we have considered. For example $\sigma \sim -354r_h^2$ is the maximum value for $l = 1$ at frequency $k \sim 0.1r_h^{-1}$ at $r_{\text{int}} \sim 25r_h$. In the perturbative framework, the scatter solution of a particular order depends on the GW background and lower order EM solution as the source. Particularly when the maximum amplitude of the lower order EM solution appears away from the BH, GW amplitude is always maximum near the horizon. The resultant of those two contributing factors effectively decides the location of the interaction surface for which superradiant amplitude is maximized. This is reminiscent of much studied [42, 49] superradiance from rotating BHs whose effective potential maximizes itself a little away from the event horizon.

In fig.3 we have shown the behaviour of the superradiant absorption cross section with different frequencies. Like the usual case of static charged or rotating BHs [27], a ringing BH also exhibits superradiance at low frequency with distinct time varying features induced by the GWs. We have obtained the expected cut-off frequency beyond which the superradiance ceases to exist for different angular momentum (l). For example, we obtain $k_{\text{max}} = 0.28r_h^{-1}$ for $l = 1$ above which superradiance vanishes, and similarly for $l = 2, k_{\text{max}} \sim 0.55r_h^{-1}$, and $l = 3, k_{\text{max}} \sim 0.8r_h^{-1}$. A non-trivial point to note is that for the higher angular momentum mode the cut-off frequency k_{max} increases contrary to the usual expectation as exciting higher frequency mode would be difficult. For example, only long wavelength modes are amplified in the usual superradiance phenomena from black hole [25–29]. For the ringing case, however, the reason could be due to complicated mode coupling and their competition in the source terms (see details in the Appendix.A). Our result seems to suggest that the perturbative scheme may not be valid above certain angular modes which could be further inferred from the increasing superradiant amplitude for higher angular mode l shown in Fig.3. However, this is not a unique feature to the ringing case, for the

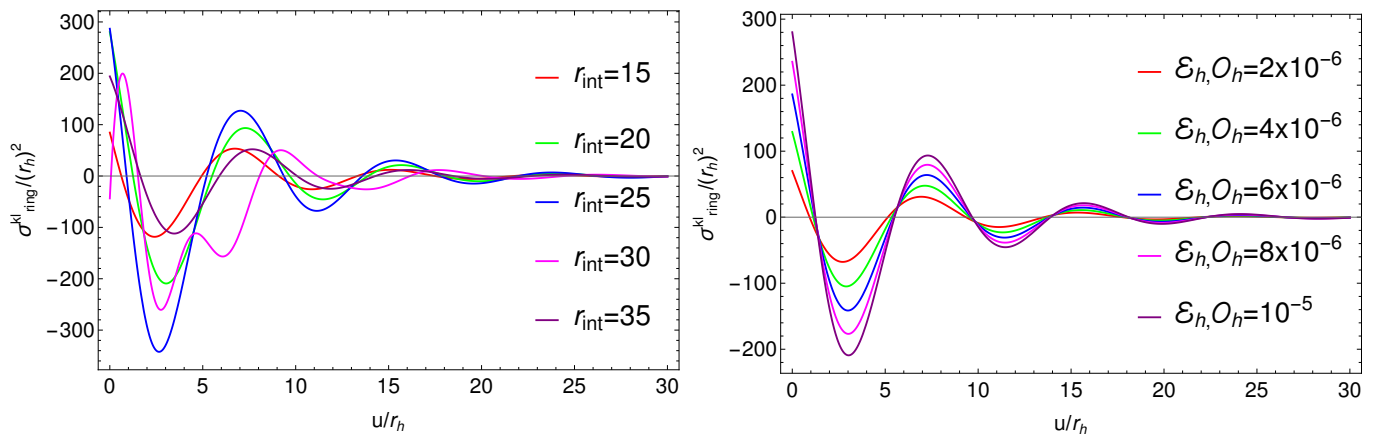


FIG. 2. On the left panel absorption cross section of the ringing BH for the EM field has been plotted with time, u , for various interaction surfaces, r_{int} , considering frequency, $k = 0.1r_h^{-1}$ and $l = 1$. On the right panel, we have plotted the same by varying the background amplitude, $\mathcal{E}_h, \mathcal{O}_h$, considering frequency, $k = 0.1r_h^{-1}$ and $l = 1$ at a particular interaction surface $r_{int} = 20r_h$. All the parameters written inside the plots are in units of r_h .

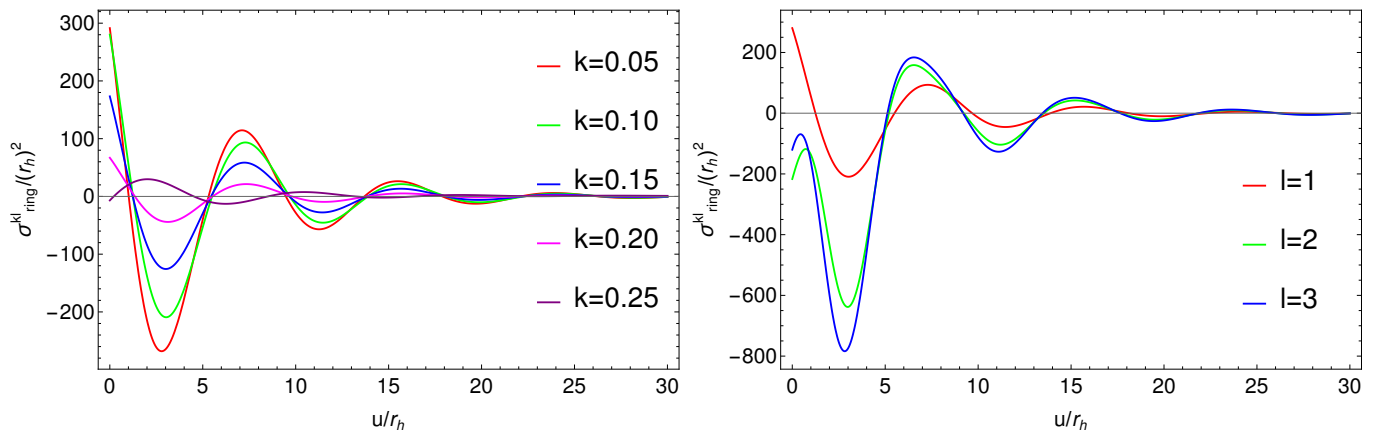


FIG. 3. On the left panel absorption cross section of the ringing black hole for the EM field has been plotted with time, u , by varying the frequency, k , of the EM field considering $l = 1$. On the right panel, we have plotted the same various angular modes, l , of the EM field considering $k = 0.1r_h^{-1}$. All the parameters written inside the plots are in units of r_h .

moving BH system similar behaviour in the absorption cross-section has been observed shown in [30]. Nonetheless, further details need to be investigated to decode such behaviour, and that is beyond the scope of our present study.

VII. OBSERVABILITY

The evaluated flux of EM waves with enhanced amplitude could be detected in low frequency ground-based observatories. From our analysis, the cutoff frequency for the occurrence of superradiance turned out to be, $\omega \sim 10^5 k_{\max} (M_{\odot}/M)$ Hz, where, M_{\odot} is the solar mass and M is the BH mass under consideration. Whereas, k_{\max} is the dimensionless cutoff frequency discussed before. As an example for a solar mass BH, with EM field parameters $l = 1$, $k_{\max} = 0.28$, we obtain $\omega \sim 10^4$ Hz in

the very low radio frequency range below which we would expect to observe the superradiant scattering.

The Existing ground-based observatories such as LO-FAR (Low Frequency Array), are sensitive to the EM wave within the frequency band, 10 – 240 MHz, or wavelength $\sim 30 - 1.2m$ [50, 51]. Converting this experimental range of frequency in our present context, we obtain the required BH mass range would be within $M \sim 10^{-2} - 10^{-1} M_{\odot}$, from which superradiant scattering of EM field could be relevant for detection. However, the smallest compact object in the binary coalescence found by LIGO, VIRGO [11] is $M \sim 2.6 M_{\odot}$, which falls in the mass gap region of a neutron star and very light black hole. Further, for the astrophysical BHs, the lower limit of mass is set by Chandrasekhar limit $M \sim 1.4 M_{\odot}$ [52, 53]. Therefore, to be able to observe any superradiant scattering of the EM field, the required mass of the BHs should not be of astrophysical origin. The interest-

ing way out appears to be primordial BHs (PBHs) which have garnered a lot of interest in the recent past, particularly in cosmology [54, 55]. At this point, we should mention there are some interesting studies already [56–58] on superradiance from PBHs.

PBHs are assumed to form due to gravitational collapse during the usual cosmological evolution if the density perturbation is very large in some spatial region (details of the formation mechanism can be found in [59–62] and for observational perspective [63, 64]). If the universe is radiation-dominated, and density perturbation satisfies the appropriate condition, the PBH formation mass can be estimated from [62]

$$M \sim M_{\text{pl}}^2 H^{-1} \quad (28)$$

where the Hubble radius $H = \sqrt{\rho_r/3M_{\text{pl}}^2}$, M_{pl} is the reduced Planck mass. Whereas, radiation energy density $\rho_r = (\pi^2 g_*/30)T^4$. T is the radiation temperature and g_* is the effective number of relativistic degrees of freedom. Utilizing these expressions we can estimate the early universe temperature when a BH of particular mass is formed, $T^2 \sim M_{\text{pl}}^3 \sqrt{90/(\pi^2 g_*)}/M$. For example the BH of mass $M \sim 10^{-2}M_\odot$ at present is formed when the temperature of the universe was $T \sim 128$ GeV. If we have a large number of such PBHs formed in the early epoch of the universe, their merger can go through the ringing phase leading to superradiant amplification within the detectable range of frequency as mentioned. Moreover, it can be shown that if the PBHs mass $M \lesssim 10^{15}$ gram, those will evaporate by now given the age of the universe $\sim 10^9 \text{yr}$ [65–67]. Therefore, in principle, one can extend the mass range of the PBH within $10^{-1}M_\odot > M > 10^{-18}M_\odot$, that can survive till now and merge. Depending upon their merger rate and distribution, they can in principle lead to superradiant scattering within a wide observable frequency range $10^6 \text{ Hz} < \omega < 10^{22} \text{ Hz}$. However, important to note that cross-section being $\sigma \propto r_h^2 \propto M^2$, lowering the mass naturally reduces the superradiant signal strength. Therefore, BH mass within the range $M \sim 10^{-1}M_\odot - 10^{-2}M_\odot$ could be of importance from the observational point of view. Several ground-based radio observatories are fully operational to explore EM signals, such as the Giant Metrewave Radio Telescope (GMRT) with frequency range, $\omega \gtrsim 50\text{MHz}$ [68–70], Square Kilometer Array (SKA)[71], and Very Large Array (VLA) [72] other than LOFAR (already mentioned). Moreover, the latest addition, LOTAAS (LOFAR Tied-Array All-Sky Survey)[73–76] is capable of receiving signals throughout the northern hemisphere.

To this end, we must point out the time scale of the evolving superradiant amplitude $\tau \sim 200(M/M_\odot)\mu\text{s}$ which is of the order of GW oscillation time scale. Therefore, to measure such a signal the sensitivity in the time measurement is extremely important, and in this range with, $M \sim 10^{-2}M_\odot$, implying $\tau \sim 2\mu\text{s}$, only LOFAR with precision $\sim 0.1 \text{ ns}$ [51], could detect those. To put

Observatory	Frequency range	Precision time
LOFAR	10 – 240MHz	$\sim 0.1\text{ns}$
GMRT	50MHz – 1.5GHz	$\sim 81\mu\text{s}$
VLA	74MHz - 50GHz	$\sim 5\text{ms}$
BH mass range	Superradiant frequency	$\sigma_{\text{ring}}^{kl}$ time scale (τ)
$0.1M_\odot - 0.01M_\odot$	1MHz – 10MHz	$20\mu\text{s} - 2\mu\text{s}$

TABLE I. The frequency and precision-time-scale of existing observatories along with the same quantities corresponding to EM absorption cross-section for a particular range of detectable BH mass range

the above estimates in perspective, in the Table.I we provide the frequency range and precision-time-scale of the existing observatories along with the frequency ranges corresponding to superradiant absorption cross-section and its oscillation time scale, (τ) for a range of BH mass. Our findings may open up an enormous opportunity to explore the prospect of direct detection of the superradiance phenomena, and a new way of observing the PBHs of cosmological origin.

VIII. CONCLUSION

To summarize, we have achieved superradiant scattering for the EM field during the ringing phase of the black hole. Unlike the static case, GW induced superradiance phenomena are transient in nature and the time scale is directly proportional to the GW oscillation time scale. We have interpreted the negative values of the absorption cross section during the course of its fast evolution as superradiant scattering. *Our analysis reveals that superradiance phenomena arise not only in the presence of rotating horizon [77], EM wave scattered through the ringing fluctuation of BH can also undergo superradiant enhancement.* Detecting the BH superradiance itself is difficult because of its extremely weak signal. GW induced time varying superradiance signal, in principle, should be easier to detect than the static one. For such a case, though, the challenge arises due to its very short time scale of oscillation. We further would like to point out that BH-BH or BH-Neutron star mergers detected by LIGO, Virgo and KAGRA [1–15] should have produced such transient superradiant EM signals. However, due to their mass $> M_\odot$ the wavelength of the signal they produced is very large of $\gtrsim 10 \text{ km}$, and observing such EM waves is far from any present day experimental limit. This immediately suggests us to look for the BH mass which should be very low $M < M_\odot$ and consequently they can produce a detectable superradiant signal in the radio or higher frequency range. Interestingly those mass ranges should be of primordial origin that has gained widespread interest in the recent past as an alternative to dark matter candidate. We found within the existing experimental setup LOFAR may have the potential to detect such a radio signal within its existing

sensitivity limit.

To this end, we must reiterate the significance of our outcome which is its complementary nature as a potential observable signature of the ringdown phase of BHs. Along with our previous findings for the scalar field [20], the effect on the EM field discussed in the present paper establishes a generic feature of the ringing black holes of

having the superradiant scattering of any fundamental field. In our future publication, we would like to take up those along with their direct detection prospects.

Acknowledgments: We would like to thank our Gravity and High Energy Physics groups at IIT Guwahati for useful discussions in several contexts. RK wants to thank Md Riajul Haque for the discussions regarding PBH.

Appendix A: Source terms in the nonhomogeneous differential equations of the EM field

In this section, we discuss elaborately the following set of equations, mentioned (8) in the main text

$$\begin{aligned}\mathcal{L}_s\chi_1^{lm} + \sum_{c\gamma} \mathcal{Q}_{lmc\gamma}^i(h)\chi_i^{c\gamma} + \sum_{c\gamma} \bar{\mathcal{Q}}_{lmc\gamma}^i(h^*)\chi_i^{c\gamma} &= 0 \\ \mathcal{L}_s\chi_2^{lm} + \sum_{c\gamma} \mathcal{R}_{lmc\gamma}^i(h)\chi_i^{c\gamma} + \sum_{c\gamma} \bar{\mathcal{R}}_{lmc\gamma}^i(h^*)\chi_i^{c\gamma} &= 0\end{aligned}\tag{A1}$$

The expression for the source terms $\mathcal{Q}_{lmc\gamma}^i(h)\chi_i^{c\gamma}$ can be expressed as

$$\mathcal{Q}_{lmc\gamma}^i(h)\chi_i^{c\gamma} = \partial_r(E_0) - \frac{1}{f(r)}\partial_t(E_1)\tag{A2}$$

where, E_0 and E_1 have the following structure:

$$\begin{aligned}E_0 &= \frac{e^{-i\omega t}}{2} \left[\Lambda_{c\gamma lm}^{(0,0)} \left\{ -f(r)c(c+1)\chi_1^{c\gamma}(-2h_1^{(e)}(2\sqrt{5})) + \frac{1}{r^2}\partial_t\chi_2^{c\gamma}h_2(2\sqrt{5})c(c+1) - \chi_4^{c\gamma}Gc(c+1)2\sqrt{5} \right. \right. \\ &+ \left. \frac{1}{r^2}\partial_t\chi_2^{c\gamma}h_2\frac{3}{2}\sqrt{\frac{5}{\pi}}4\gamma\frac{\pi}{3}\frac{1}{\sqrt{4\pi}} \right\} \\ &+ \Lambda_{c\gamma lm}^{(1,0)} \left\{ i\gamma\partial_t\chi_2^{c\gamma} \left(-2(H+G)\sqrt{15} - 2G\frac{3}{2}\sqrt{\frac{5}{\pi}} \left(2\gamma\sqrt{\frac{\pi}{3}} \right) \right) - 2f(r)\partial_t\chi_2^{c\gamma}(-i\gamma\partial_r h_1^{(e)}\sqrt{15}) \right. \\ &- f(r) \left(-c(c+1)\partial_r\chi_1^{c\gamma}(2(K-3G)) - 2\partial_r\chi_4^{c\gamma}(-i\gamma h_1^{(o)}\sqrt{15}) - 2\chi_4^{c\gamma}(-i\gamma\partial_r h_1^{(o)}\sqrt{15}) \right. \\ &- 2i\gamma H_1\partial_r\chi_2^{c\gamma}\sqrt{15} + c(c+1)\chi_1^{c\gamma}2h_1^{(o)}(-i\gamma\sqrt{15}) + 2\partial_t\partial_r\chi_2^{c\gamma}(-h_1^{(e)}\sqrt{15}) \left. \right) \\ &- \left. \chi_4^{c\gamma}h_2 \left(3i\gamma\sqrt{15} + 2i\gamma2\gamma\sqrt{\frac{\pi}{3}}\frac{3}{2}\sqrt{\frac{5}{\pi}} - i\gamma\frac{3}{2}\sqrt{\frac{5}{\pi}}2\sqrt{\frac{\pi}{3}} \right) \right\} \\ &+ \Lambda_{c\gamma lm}^{(2,0)} \left\{ -f(r) \left(-c(c+1)\chi_1^{c\gamma}\partial_r(2(K-3G)) + c(c+1)\chi_1^{c\gamma}4h_1^{(e)} + 2\chi_3^{c\gamma}H_1c(c+1) \right) \right. \\ &- \left. \chi_4^{c\gamma} \left(-2c(c+1)H - 2Gc(c+1) \right) + \frac{1}{r^2}\partial_t\chi_2^{c\gamma}h_2 \left(-2c(c+1) + \frac{3}{2}\sqrt{\frac{5}{\pi}}4\gamma\frac{\pi}{3}\frac{2}{\sqrt{20\pi}} \right) \right\} \\ &+ \bar{\Lambda}_{c\gamma lm}^{(2,0)} \left\{ -f(r) \left(-2\partial_r\chi_4^{c\gamma}h_1^{(e)} - 2\chi_4^{c\gamma}\partial_r h_1^{(e)} + c(c+1)\chi_1^{c\gamma}2h_1^{(o)} - 2\chi_3^{c\gamma}H_1 - 4\partial_t\partial_r\chi_2^{c\gamma}h_1^{(o)} + 2\partial_t\chi_2^{c\gamma}(-\partial_r h_1^{(o)}) \right) \right. \\ &- \left. \chi_4^{c\gamma}2(H+G) + 3\frac{1}{r^2}\partial_t\chi_2^{c\gamma}h_2 \right\} \\ &+ \frac{1}{r^2}\partial_t\chi_2^{c\gamma}h_2 \left\{ \frac{3}{2}\sqrt{\frac{5}{\pi}} \left(\frac{2}{3}\sqrt{2\pi}\sqrt{(c-\gamma)(c+\gamma+1)}\frac{1}{\sqrt{4\pi}}\Lambda_{c\gamma+1lm}^{(2,-1)} \right) \right\} + \frac{1}{r^2}\chi_4^{lm}G2m^2\frac{3}{2}\sqrt{\frac{5}{\pi}} \end{aligned}\tag{A3}$$

and,

$$\begin{aligned}
E1 = & \frac{e^{-i\omega t}}{2} \left[\Lambda_{c\gamma lm}^{(0,0)} \left\{ -\partial_r \chi_2^{c\gamma} f(r) \frac{h_2}{r^2} \frac{3}{2} \sqrt{\frac{5}{\pi}} 4(\gamma - c(c+1)) \frac{\pi}{3} \frac{1}{\sqrt{4\pi}} \right. \right. \\
& + 2\chi_2^{c\gamma} \left(-c(c+1)f(r) \frac{h_1^{(o)}}{r^2} (\sqrt{5}) + c(c+1)2\sqrt{\frac{\pi}{3}} f(r) \frac{h_1^{(o)}}{r^2} \sqrt{15} \left(\frac{1}{\sqrt{4\pi}} \right) + f(r)G \frac{3}{2} \sqrt{\frac{5}{\pi}} \left(-\chi_3^{c\gamma} c(c+1)4 \frac{\pi}{3} \frac{1}{\sqrt{4\pi}} \right) \right\} \\
& + \Lambda_{c\gamma lm}^{(1,0)} \left\{ 2\chi_4^{c\gamma} \gamma \omega h_1^{(o)} \sqrt{15} - \partial_r \chi_2^{c\gamma} f(r) 2i\gamma (H - G) \sqrt{15} + 2(-ik)\chi_4^{c\gamma} i\gamma h_1^{(o)} \sqrt{15} - \partial_t \chi_2^{c\gamma} (-2H_1 \sqrt{15} i\gamma + 2\gamma \omega h_1^{(e)} \sqrt{15}) \right. \\
& + \partial_t^2 \chi_2^{c\gamma} (-2i\gamma h_1^{(e)} \sqrt{15}) + 2\chi_2^{c\gamma} (-c(c+1)i\gamma f(r) h_1^{(e)} \sqrt{15}) + \chi_3^{c\gamma} f(r) i\gamma \frac{h_2}{r^2} \left(-2\sqrt{\frac{\pi}{3}} \frac{3}{2} \sqrt{\frac{5}{\pi}} + 3\sqrt{15} - 2\frac{3}{2} \sqrt{\frac{5}{\pi}} (2\gamma \sqrt{\frac{\pi}{3}}) \right) \\
& + f(r)G \frac{3}{2} \sqrt{\frac{5}{\pi}} 2i\gamma \partial_r \chi_2^{c\gamma} 2\gamma \sqrt{\frac{\pi}{3}} \left. \right\} + \Lambda_{c\gamma+1lm}^{(1,-1)} \left(2\sqrt{\frac{2\pi}{3}} \sqrt{(c-\gamma)(c+\gamma+1)} \right) \left\{ i\gamma \chi_3^{c\gamma} f(r) \frac{h_2}{r^2} + 2i\gamma f(r)G \partial_r \chi_2^{c\gamma} \frac{3}{2} \sqrt{\frac{5}{\pi}} \right\} \\
& + \Lambda_{c\gamma lm}^{(2,0)} \left\{ 2\chi_4^{c\gamma} H_1 (-c(c+1)) - \partial_r \chi_2^{c\gamma} f(r) \frac{h_2}{r^2} \frac{3}{2} \sqrt{\frac{5}{\pi}} 4(\gamma - c(c+1)) \frac{\pi}{3} \frac{1}{\sqrt{4\pi}} + 2\chi_2^{c\gamma} \left(-c(c+1)f(r) \frac{h_1^{(o)}}{r^2} (-4) \right. \right. \\
& + c(c+1)2\sqrt{\frac{\pi}{3}} f(r) \frac{h_1^{(o)}}{r^2} \sqrt{15} \left(\frac{2}{\sqrt{20\pi}} \right) + \chi_3^{c\gamma} f(r) (2Hc(c+1)) + 2(K - 3G) (i\omega c(c+1)\chi_1^{c\gamma} - c(c+1)\partial_t \chi_1^{c\gamma}) \\
& + f(r)G \frac{3}{2} \sqrt{\frac{5}{\pi}} \left(-\chi_3^{c\gamma} c(c+1)4 \frac{\pi}{3} \frac{2}{\sqrt{20\pi}} \right) \left. \right\} - \Lambda_{c\gamma+1lm}^{(2,-1)} \partial_r \chi_2^{c\gamma} f(r) \frac{h_2}{r^2} \frac{3}{2} \sqrt{\frac{5}{\pi}} \left(\frac{2}{3} \sqrt{2\pi} \sqrt{(c-\gamma)(c+\gamma+1)} \frac{1}{\sqrt{4\pi}} \right) \\
& + \tilde{\Lambda}_{c\gamma lm}^{(2,0)} \left\{ 2\chi_4^{c\gamma} H_1 + 2\chi_4^{c\gamma} i\omega h_1^{(e)} - 2\partial_t \chi_4^{c\gamma} h_1^{(e)} - \partial_r \chi_2^{c\gamma} 3f(r) \frac{h_2}{r^2} - \partial_t \chi_2^{c\gamma} \{-2i\omega h_1^{(o)}\} + \partial_t^2 \chi_2^{c\gamma} (-2h_1^{(o)}) \right. \\
& + 2\chi_2^{c\gamma} \left(-c(c+1)f(r) \frac{h_1^{(o)}}{r^2} \right) + \chi_3^{c\gamma} f(r) (-2H + 2G) \left. \right\} \\
& + f(r)G \frac{3}{2} \sqrt{\frac{5}{\pi}} \chi_3^{lm} (-2m^2 + l(l+1)) + \partial_r \chi_2^{lm} f(r) \frac{h_2}{r^2} \frac{3}{2} \sqrt{\frac{5}{\pi}} (2m^2 - l(l+1)) \left. \right] \tag{A4}
\end{aligned}$$

Given the expression for $\mathcal{Q}_{lmc\gamma}^i(h)\chi_i^{c\gamma}$, one can derive the contribution $\bar{\mathcal{Q}}_{lmc\gamma}^i(h^*)\chi_i^{c\gamma}$ coming from the complex conjugate part of the background metric by simply taking the conjugate of every metric coefficients that appeared in the previous equation for (A2). As a consequence, we also have a 1/2 factor in front of every source term. We have made use of Wigner-3j symbols repeatedly as can be seen from the equations, with the main definition given as

$$Y_l^m(\theta, \phi) Y_{l'}^{m'}(\theta, \phi) = \sum_{c\gamma} \Lambda_{lmc\gamma}^{(l', m')} Y_c^\gamma(\theta, \phi) \tag{A5}$$

where,

$$\Lambda_{lmc\gamma}^{(l', m')} = (-1)^\gamma \sqrt{\frac{(2l'+1)(2l+1)}{4\pi}} \sqrt{2c+1} \begin{pmatrix} l & l' & c \\ m & m' & -\gamma \end{pmatrix} \begin{pmatrix} l & l' & c \\ 0 & 0 & 0 \end{pmatrix}.$$

For the non-zero value of the Wigner 3j coefficient $\begin{pmatrix} l & l' & c \\ m & m' & -\gamma \end{pmatrix}$, all the l values should satisfy the triangle law; the sum of any two l should be greater than equal to the third one and the sum of all the m values should be zero. Some other mathematical quantities we need in the following discussion, constructed out of $\Lambda_{lmc\gamma}^{(l', m')}$, are

$$\begin{aligned}
S_{lmc\gamma} & \equiv 2m \sqrt{\frac{\pi}{3}} \sum_{c\gamma} \Lambda_{lmc\gamma}^{(1,0)} + 2\sqrt{\frac{2\pi}{3}} \sqrt{(l-m)(l+m+1)} \Lambda_{lm+1c\gamma}^{(1,-1)} \\
\tilde{S}_{lmc\gamma} & \equiv \frac{m}{3} \sqrt{4\pi} \Lambda_{lmc\gamma}^{(0,0)} + \frac{2m}{3} \sqrt{\frac{4\pi}{5}} \Lambda_{lmc\gamma}^{(2,0)} + 4\sqrt{2} \frac{\pi}{3} \sqrt{(l-m)(l+m+1)} \frac{1}{\sqrt{4\pi}} \Lambda_{lm+1c\gamma}^{(2,-1)} \\
\tilde{\Lambda}_{lmc\gamma}^{(2,0)} & \equiv - \left[2m \Lambda_{lmc\gamma}^{(2,0)} + m\sqrt{5} \Lambda_{lmc\gamma}^{(0,0)} + \sqrt{(l-m)(l+m+1)} 3\sqrt{\frac{2}{3}} \Lambda_{lm+1c\gamma}^{(2,-1)} \right] \tag{A6}
\end{aligned}$$

For the source terms in the equation (A1) governing χ_2^{lm} , we have,

$$\begin{aligned}
\mathcal{R}_{lmc\gamma}^i(h)\chi_i^{c\gamma} &= \frac{e^{-i\omega t}}{2} \left[\Lambda_{c\gamma lm}^{(0,0)} \left\{ \chi_3^{c\gamma} \left(-\frac{2f(r)h_2}{r^3} + \frac{(h_2f'(r) + f(r)\partial_r h_2)}{r^2} \right) 2\sqrt{5}\gamma(\gamma+1) \right. \right. \\
&+ \chi_3^{c\gamma} \frac{2f(r)h_1^{(o)}}{r^2} 2\gamma(\gamma+1)\sqrt{5} + \partial_r \chi_3^{c\gamma} \frac{f(r)h_2}{r^2} 2\sqrt{5}\gamma(\gamma+1) + \chi_4^{lm} \frac{i\omega}{r^2 f(r)} h_2 2\sqrt{5}\gamma(\gamma+1) \\
&+ ik\chi_4^{c\gamma} \frac{1}{r^2 f(r)} h_2 2\sqrt{5}\gamma(\gamma+1) - \left(2i\omega \frac{\gamma(\gamma+1)}{r^2} \chi_1^{c\gamma}(t,r) - \frac{\gamma(\gamma+1)}{r^2} \partial_t \chi_1^{c\gamma}(t,r) \right) h_1^{(o)} (\sqrt{10} - \sqrt{5}) \\
&- \chi_2^{c\gamma}(t,r) 2\gamma(\gamma+1) \left(\frac{2}{r^3} f(r) h_1^{(e)} - \frac{1}{r^2} \partial_r h_1^{(e)} - \frac{1}{r^2} h_1^{(e)} f'(r) \right) (\sqrt{10} - \sqrt{5}) + \chi_2^{c\gamma}(t,r) \gamma(\gamma+1) \frac{1}{r^2} 2(K-3G) (\sqrt{10} - \sqrt{5}) \\
&+ \partial_r \chi_2^{lm}(t,r) \left(f'(r) l(l+1) 2G\sqrt{5} - f(r) \frac{1}{r^2} 2h_1^{(e)} 2l(l+1)\sqrt{5} + f(r) \frac{1}{r^2} 2l(l+1)h_1^{(e)} (\sqrt{10} - \sqrt{5}) - 4i\omega H_1 l(l+1)\sqrt{5} \right) \\
&+ \partial_r^2 \chi_2^{lm}(t,r) f(r) l(l+1) 2G\sqrt{5} \left. \right\} \\
&+ \Lambda_{c\gamma lm}^{(1,0)} \left\{ 2\gamma\omega H_1 \sqrt{15} \chi_3^{c\gamma}(t,r) - 6f(r) i\gamma \sqrt{\frac{5}{3}} \partial_r G \chi_3^{c\gamma}(t,r) - f'(r) 2G \sqrt{15} i\gamma \chi_3^{c\gamma}(t,r) - 2(Hf'(r) + f(r)\partial_r H) i\gamma \sqrt{15} \chi_3^{c\gamma}(t,r) \right. \\
&+ \frac{2f(r)h_1^{(e)}}{r^2} (2+l(l+1)) \sqrt{15} i\gamma \chi_3^{c\gamma}(t,r) - f(r) 2G \sqrt{15} i\gamma \partial_r \chi_3^{c\gamma}(t,r) - f(r) 2\sqrt{15} H i\gamma \partial_r \chi_3^{c\gamma}(t,r) - \chi_4^{c\gamma}(t,r) 2i\gamma \sqrt{15} \partial_r H_1 \\
&- 2\chi_4^{c\gamma}(t,r) \sqrt{15} \frac{\gamma\omega}{f(r)} (H-G) + \sqrt{15} 2im H_1 \partial_r \chi_4^{lm}(t,r) + 2G \sqrt{15} i\gamma \partial_t \chi_4^{c\gamma}(t,r) \\
&+ \left(2i\omega \frac{\gamma(\gamma+1)}{r^2} \chi_1^{c\gamma}(t,r) - \frac{\gamma(\gamma+1)}{r^2} \partial_t \chi_1^{c\gamma}(t,r) \right) \sqrt{15} i\gamma h_1^{(e)} - \left(\frac{2f(r)h_1^{(e)}}{r^3} - \frac{(h_1^{(e)} f'(r) + f(r)\partial_r h_1^{(e)})}{r^2} \right) \sqrt{15} i\gamma \chi_2^{c\gamma}(t,r) \\
&+ \partial_r \chi_2^{c\gamma}(t,r) \left(-\frac{2f(r)h_2}{r^3} + \frac{(h_2f'(r) + f(r)\partial_r h_2)}{r^2} \right) 2\sqrt{15} i\gamma + 2\partial_r \chi_2^{c\gamma}(t,r) f(r) \frac{1}{r^2} h_1^{(o)} \left((2+l(l+1)) \sqrt{15} i\gamma + \sqrt{15} l(l+1) i\gamma \right) \\
&+ \partial_r^2 \chi_2^{c\gamma}(t,r) f(r) \frac{1}{r^2} h_2 2\sqrt{15} i\gamma + \partial_t \chi_2^{c\gamma}(t,r) i\omega \frac{h_2}{r^2 f(r)} 2\sqrt{15} i\gamma - \partial_t^2 \chi_2^{c\gamma}(t,r) \frac{1}{r^2 f(r)} h_2 2\sqrt{15} i\gamma \left. \right\} \\
&+ \Lambda_{c\gamma lm}^{(2,0)} \left\{ -2\chi_3^{c\gamma}(t,r) \left(-\frac{2f(r)h_2}{r^3} + \frac{(h_2f'(r) + f(r)\partial_r h_2)}{r^2} \right) \gamma(\gamma+1) - 8\chi_3^{c\gamma}(t,r) \frac{2f(r)h_1^{(o)}}{r^2} l(l+1) \right. \\
&- 2\partial_r \chi_3^{c\gamma}(t,r) \frac{f(r)h_2}{r^2} \gamma(\gamma+1) - \chi_4^{c\gamma}(t,r) \frac{i\omega}{r^2 f(r)} h_2 2\gamma(\gamma+1) + \partial_t \chi_4^{c\gamma}(t,r) \left(-\sqrt{15} \frac{i\gamma}{f(r)} 2Hr^2 + \frac{1}{r^2 f(r)} h_2 2\gamma(\gamma+1) \right) \\
&- \left(2i\omega \frac{\gamma(\gamma+1)}{r^2} \chi_1^{c\gamma}(t,r) - \frac{\gamma(\gamma+1)}{r^2} \partial_t \chi_1^{c\gamma}(t,r) \right) h_1^{(o)} (2\sqrt{2} + 4) \\
&+ \chi_2^{c\gamma}(t,r) \left(-2\gamma(\gamma+1) \left(\frac{2}{r^3} f(r) h_1^{(e)} - \frac{1}{r^2} \partial_r h_1^{(e)} - \frac{1}{r^2} h_1^{(e)} f'(r) \right) (2\sqrt{2} + 4) + l(l+1) \frac{1}{r^2} 2(K-3G) (2\sqrt{2} + 4) \right) \\
&+ \partial_r \chi_2^{c\gamma}(t,r) \left(-\gamma(\gamma+1) f'(r) H(r) + \gamma(\gamma+1) 2G + f(r) \frac{1}{r^2} 2h_1^{(e)} 8\gamma(\gamma+1) + f(r) \frac{1}{r^2} 2\gamma(\gamma+1) h_1^{(e)} (2\sqrt{2} + 4) \right. \\
&+ 2i\omega H_1 8\gamma(\gamma+1) \left. \right) - \partial_r^2 \chi_2^{c\gamma}(t,r) f(r) \gamma(\gamma+1) 2G - \partial_t \chi_2^{c\gamma}(t,r) \left(-2\partial_r H_1 \gamma(\gamma+1) - i\omega \frac{1}{f(r)} 2\gamma(\gamma+1) (H-G) \right) \\
&+ \partial_t^2 \chi_2^{c\gamma}(t,r) \frac{1}{f(r)} \gamma(\gamma+1) 2(G-H) + 4\partial_t \partial_r \chi_2^{c\gamma}(t,r) H_1 \gamma(\gamma+1) \left. \right\} \\
&+ \tilde{\Lambda}_{c\gamma lm}^{(2,0)} \left\{ 2\chi_3^{c\gamma}(t,r) \left(-\frac{2f(r)h_2}{r^3} + \frac{(h_2f'(r) + f(r)\partial_r h_2)}{r^2} \right) - \chi_3^{c\gamma}(t,r) \frac{2f(r)h_1^{(o)}}{r^2} 2\gamma(\gamma+1) (3 + \gamma(\gamma+1)) \right. \\
&+ 2\partial_r \chi_3^{c\gamma}(t,r) \frac{f(r)h_2}{r^2} + 2\chi_4^{c\gamma}(t,r) \frac{i\omega}{r^2 f(r)} h_2 - 2\partial_t \chi_4^{c\gamma}(t,r) \frac{1}{r^2 f(r)} h_2 + \left(2i\omega \frac{\gamma(\gamma+1)}{r^2} \chi_1^{c\gamma}(t,r) - \frac{\gamma(\gamma+1)}{r^2} \partial_t \chi_1^{c\gamma}(t,r) \right) h_1^{(o)} \\
&+ \chi_2^{c\gamma}(t,r) \left(2\gamma(\gamma+1) \left(\frac{2}{r^3} f(r) h_1^{(e)} - \frac{1}{r^2} \partial_r h_1^{(e)} - \frac{1}{r^2} h_1^{(e)} f'(r) \right) - \gamma(\gamma+1) \frac{1}{r^2} 4(K-3G) \right. \\
&+ \partial_r \chi_2^{c\gamma}(t,r) \left(f'(r) H(r) + f'(r) 2G - f(r) \frac{1}{r^2} 2h_1^{(e)} (3 + \gamma(\gamma+1)) - f(r) \frac{1}{r^2} 2l(l+1) h_1^{(e)} - f(r) 2\partial_r (K-3G) \right. \\
&- 2i\omega H_1 (3 + \gamma(\gamma+1)) \left. \right) + \partial_r^2 \chi_2^{c\gamma}(t,r) \left(f(r) 2G + 2f(r) H \right) - \partial_t \chi_2^{c\gamma}(t,r) \left(2\partial_r H_1 + i\omega \frac{1}{f(r)} 2(H-G) \right) \\
&+ \partial_t^2 \chi_2^{c\gamma}(t,r) \frac{1}{f(r)} 2(H-G) - 4\partial_t \partial_r \chi_2^{c\gamma}(t,r) H_1 \left. \right\}
\end{aligned}$$

$$\begin{aligned}
& + S_{c\gamma lm} \left\{ \chi_3^{c\gamma}(t, r) \left(-f'(r) 3i\gamma G \sqrt{\frac{5}{\pi}} + \frac{2f(r)h_1^{(e)}}{r^2} 3\sqrt{\frac{5}{\pi}} i\gamma \right) - \partial_r \chi_3^{c\gamma}(t, r) f(r) \left(3i\gamma G \sqrt{\frac{5}{\pi}} \right) + \partial_t \chi_4^{c\gamma}(t, r) \left(3i\gamma G \sqrt{\frac{5}{\pi}} \right) r^2 \right. \\
& + \partial_r \chi_2^{c\gamma}(t, r) \left(\left(-\frac{2f(r)h_2}{r^3} + \frac{(h_2 f'(r) + f(r)\partial_r h_2)}{r^2} \right) \left(3i\gamma \sqrt{\frac{5}{\pi}} \right) + 2f(r) \frac{1}{r^2} h_1^{(o)} \left(3\sqrt{\frac{5}{\pi}} i\gamma \right) \right) \\
& - \partial_r^2 \chi_2^{c\gamma}(t, r) f(r) \frac{1}{r^2} h_2 \left(-3i\gamma \sqrt{\frac{5}{\pi}} \right) - \partial_t \chi_2^{c\gamma}(t, r) i\omega \frac{h_2}{r^2 f(r)} \left(-3i\gamma \sqrt{\frac{5}{\pi}} \right) + \partial_t^2 \chi_2^{c\gamma}(t, r) \frac{1}{r^2 f(r)} h_2 \left(-3i\gamma \sqrt{\frac{5}{\pi}} \right) \left. \right\} \\
& + \tilde{S}_{c\gamma lm} \left\{ -\chi_3^{c\gamma}(t, r) \frac{2f(r)h_1^{(o)}}{r^2} 2\gamma(\gamma+1) \frac{3}{2} \sqrt{\frac{5}{\pi}} + \partial_r \chi_2^{c\gamma}(t, r) \left(-f(r) \frac{1}{r^2} 2h_1^{(e)} \frac{3}{2} \sqrt{\frac{5}{\pi}} - 2i\omega H_1 \frac{3}{2} \sqrt{\frac{5}{\pi}} \right) \right\} \\
& + \chi_3^{lm}(t, r) \left\{ \left(-\frac{2f(r)h_2}{r^3} + \frac{(h_2 f'(r) + f(r)\partial_r h_2)}{r^2} \right) \left(-3m^2 \sqrt{\frac{5}{\pi}} \right) - \frac{2f(r)h_1^{(o)}}{r^2} \left(-2l(l+1)(+3m^2 \sqrt{\frac{5}{\pi}}) \right) \right\} \\
& + \partial_r \chi_3^{lm}(t, r) \left\{ \frac{f(r)h_2}{r^2} \left(-3m^2 \sqrt{\frac{5}{\pi}} \right) \right\} + \chi_4^{lm}(t, r) \left\{ \frac{i\omega}{r^2 f(r)} h_2 \left(-3m^2 \sqrt{\frac{5}{\pi}} \right) \right\} \\
& + \partial_t \chi_4^{lm}(t, r) \left\{ -\frac{1}{r^2 f(r)} h_2 \left(-3m^2 \sqrt{\frac{5}{\pi}} \right) \right\} + \chi_2^{lm}(t, r) \left\{ -l^2(l+1)^2 2(K-3G) \right\} \left. \right\} \\
& + \partial_r \chi_2^{lm}(t, r) \left\{ +2(f(r)H'(r) - f(r) \left(-2l(l+1)\partial_r(K_3G) \right) - f'(r)3m^2G \sqrt{\frac{5}{\pi}} + f(r) \frac{1}{r^2} 2h_1^{(e)} \left(3m^2 \sqrt{\frac{5}{\pi}} \right) \right. \right. \\
& \left. \left. + 2i\omega H_1 \left(+3m^2 \sqrt{\frac{5}{\pi}} \right) \right) \right\} + \partial_r^2 \chi_2^{lm}(t, r) \left\{ -f(r) \left(3m^2 G \sqrt{\frac{5}{\pi}} \right) \right\} + \partial_t^2 \chi_2^{lm}(t, r) \left\{ \frac{1}{f(r)} \left(3m^2 G \sqrt{\frac{5}{\pi}} \right) \right\} \left. \right\}
\end{aligned} \tag{A7}$$

Given the expression for $\mathcal{R}_{lmc\gamma}^i(h)\chi_i^{c\gamma}$ one can derive the contribution $\bar{\mathcal{R}}_{lmc\gamma}^i(h)\chi_i^{c\gamma}$ in the same way described for $\bar{\mathcal{Q}}_{lmc\gamma}^i(h)\chi_i^{c\gamma}$.

Appendix B: Definition Of The Absorption Cross Section

In our framework, the procedure to determine the absorption cross section for an oscillating black hole arises from the definition followed in the case of static and stationary black holes. For this we first study the case of static and stationary black holes, and then we extend the formalism to the oscillating black hole. To proceed we write down the covariant conservation equation on a generic spacetime background with the associated Killing vector, ξ^μ , as [46],

$$\nabla_\mu (\mathcal{T}^\mu{}_\nu \xi^\nu) = 0, \tag{B1}$$

which can be explicitly checked using the covariant conservation of the symmetric stress energy tensor, $\nabla_\mu \mathcal{T}^\mu{}_\nu = 0$, and the killing equation $\nabla^\mu \xi^\nu + \nabla^\nu \xi^\mu = 0$. Let us symbolize the quantity inside the parenthesis of the above equation as the generalized four momentum, $P^\mu = \mathcal{T}^\mu{}_\nu \xi^\nu$. To determine the conserved quantity, one needs to find out the allowed Killing vectors. For example, the static spherically symmetric (Schwarzschild type black hole) spacetime, in $(u = t - r_*, r)$,

$$ds^2 = -f(r)du^2 - 2dudr + r^2 d\Omega, \tag{B2}$$

allows one of the time like Killing vectors as $\xi = \delta_0^\mu \partial_\mu$. For this particular Killing vector associated conserved quantity turns out to be

$$\mathcal{F} = \int d^3x \sqrt{-g} P^0, \tag{B3}$$

that implies, $\partial_u \mathcal{F} = 0$. Taking the time derivative on both sides of the above equation we get

$$\partial_u \mathcal{F} = \int d^3x \partial_u (\sqrt{-g} P^0) = - \int d^3x \partial_i (\sqrt{-g} P^i). \tag{B4}$$

By choosing a r-constant hypersurface and applying the divergence theorem in the above equation one will arrive at

$$\partial_u \mathcal{F} = - \int r^2 d\Omega P^r \Big|_{r_h}^\infty = - \int r^2 d\Omega \mathcal{T}^r{}_u \xi^u \Big|_{r_h}^\infty = - \left[\int r^2 d\Omega \mathcal{T}^r{}_u \Big|_{r \rightarrow \infty} - \int r^2 d\Omega \mathcal{T}^r{}_u \Big|_{r_h} \right] \equiv \partial_u \mathcal{E} \Big|_{r=r_h} - \partial_u \mathcal{E} \Big|_{r \rightarrow \infty} \tag{B5}$$

We can see that two terms in the last equality of the above equation are equal by the fact that $\partial_u \mathcal{F} = 0$ mentioned previously. Therefore, one may infer that the energy being absorbed by the black hole horizon per unit time could be equated with, $\partial_u \mathcal{F}_{r \rightarrow \infty}$. Now, the definition of the absorption cross section [45] is the amount of energy being absorbed by the black hole horizon divided by the incident energy density. We define the incident energy density as, $\partial_u \mathcal{G} = \mathcal{T}^z_u$, sometimes called energy density current [30]. Utilizing all these we obtain the absorption cross section in terms of the stress-energy tensor of the fields as,

$$\sigma = \frac{\partial_u \mathcal{F}}{\partial_u \mathcal{G}} = \frac{\int r^2 d\Omega \mathcal{T}^r_u}{\mathcal{T}^z_u} \quad (\text{B6})$$

In the following discussion, our main focus will be to calculate the incident energy density and to formulate the procedure to calculate the normalization factors. We start with a circularly polarized [44] ingoing plane wave propagating along z-direction towards the black hole as,

$$\begin{aligned} A_x(u, \mathbf{x}) &= e^{-ik(u+2z)} \\ A_y(u, \mathbf{x}) &= ie^{-ik(u+2z)}. \end{aligned} \quad (\text{B7})$$

The approach to finding out the normalization factor is to compare the incident plane wave with the asymptotic form of the field solution, which is obtained in spherical coordinates. We, therefore, need to transform the plane EM wave written in cartesian coordinate, $\mathbf{A} = A_x \hat{x} + A_y \hat{y}$, to spherical coordinate by using, $A'_\mu(x') = (\partial x^\nu / \partial x'^\mu) A_\nu(x)$ as,

$$\begin{aligned} A'_u(u, \mathbf{r}) &= A_u(u, \mathbf{x}); & A'_r(u, \mathbf{r}) &= \sin \theta e^{i\phi} A_x(u, \mathbf{x}) \\ A'_\theta(u, \mathbf{r}) &= r \cos \theta e^{i\phi} A_x(u, \mathbf{x}); & A'_\phi(u, \mathbf{r}) &= ir \sin \theta e^{i\phi} A_x(u, \mathbf{x}), \end{aligned} \quad (\text{B8})$$

where, we have used $A_z = 0$ and $A_y = iA_x$. Of course, $A_x(u, \mathbf{x})$ should be expressed in spherical coordinates using Rayleigh expansion of the spatial part of a plane wave propagating along the z-direction given by

$$e^{-ikz} = e^{-ikr \cos \theta} = \sum_{l=0}^{\infty} (2l+1) i^l j_l(kr) P_l^0(\cos \theta). \quad (\text{B9})$$

Taking the derivative with respect to θ on both sides of the above equation one can discover the following expression also

$$e^{-ikz} = e^{-ikr \cos \theta} = \sum_{l=0}^{\infty} (2l+1) i^l \frac{j_l(kr)}{ikr} \frac{\partial_\theta P_l^0(\cos \theta)}{\sin \theta}. \quad (\text{B10})$$

Where one needs to use the relation $P_l^1(\cos \theta) = -\partial_\theta P_l^0(\cos \theta)$. Finally, one obtains the components of plane EM waves for circularly polarized light in spherical coordinates as,

$$\begin{aligned} A'_u(u, \mathbf{r}) &= \sum_{lm} A_u^{lm}(u, r) Y_{lm}(\Omega) = 0 \\ A'_r(u, \mathbf{r}) &= \sum_{lm} A_r^{lm}(u, r) Y_{lm}(\Omega) = \sum_{lm} (-1)^{l+1} \delta_{m1} \sqrt{4\pi(2l+1)l(l+1)} \frac{e^{-ik(u+2r_*)}}{2k^2 r^2} Y_{lm}(\Omega) + \text{outgoing part} \\ A'_s(u, \mathbf{r}) &= -\sum_{lm} (-1)^{l+1} \delta_{m1} \sqrt{\frac{4\pi(2l+1)}{l(l+1)}} \left[i\Psi_s^{lm}(\Omega) + \Phi_s^{lm}(\Omega) \right] \frac{e^{-ik(u+2r_*)}}{2k} + \text{outgoing part} \end{aligned} \quad (\text{B11})$$

above expansions could be checked following $j_l(kr) + in_l(kr) \sim \frac{(-i)^{l+1} e^{ikr}}{kr}$, $j_l(kr) - in_l(kr) \sim \frac{i^{l+1} e^{-ikr}}{kr}$ for $r \rightarrow \infty$ or $kr \gg 1$, that implies $j_l(kr) \sim i^{l+1} \frac{e^{-ikr}}{2kr} + (-i)^{l+1} \frac{e^{ikr}}{2kr}$. Gauge invariant variables for circularly polarized light in this new gauge become

$$\begin{aligned} \sum_{lm} \tilde{\chi}_1^{klm}(u, r) Y^{lm}(\Omega) &= \sum_{lm} \frac{r^2}{l(l+1)} (\partial_u A_r^{lm} - \partial_r A_u^{lm}) \\ &= -i \sum_{lm} (-1)^{l+1} \delta_{m1} \sqrt{\frac{4\pi(2l+1)}{l(l+1)}} \frac{e^{-ik(u+2r_*)}}{2k} Y_{lm}(\Omega) + \text{out going} \end{aligned} \quad (\text{B12})$$

Also in the expansion of $A'_s(u, \mathbf{r})$ (B11) one can check that the term with $\Phi_s^{lm}(\Omega)$ does not transform, and we denote this as,

$$\sum_{lm} \tilde{\chi}_2^{klm}(u, r) \Phi_s^{lm}(\Omega) = - \sum_{lm} (-1)^{l+1} \delta_{m1} \sqrt{\frac{4\pi(2l+1)}{l(l+1)}} \frac{e^{-ik(u+2r_*)}}{2k} \Phi_s^{lm}(\Omega) + \text{out going} \quad (\text{B13})$$

(recall the $\frac{r^2}{l(l+1)}$ factor in the definition of $\tilde{\chi}_1$ from the main text).

Appendix C: Procedure To Evaluate The Normalized Incident Energy Density

With the gauge invariant variables derived in the previous section, one can deduce the normalization factors from the asymptotic form of these fields,

$$\begin{aligned} \sum_{lm} \tilde{\chi}_1^{klm}(u, r) Y^{lm}(\Omega) &= \sum_{lm} \mathcal{N}_1^{klm} [\mathcal{I}_1(u) e^{-ik(u+2r_*)} + \mathcal{R}_1(u) e^{-iku}] Y_{lm}(\Omega), \\ \sum_{lm} \tilde{\chi}_2^{klm}(u, r) \Phi_s^{lm}(\Omega) &= \sum_{lm} \mathcal{N}_2^{klm} [\mathcal{I}_2(u) e^{-ik(u+2r_*)} + \mathcal{R}_2(u) e^{-iku}] \Phi_s^{lm}(\Omega). \end{aligned} \quad (\text{C1})$$

Comparing with (B12) we fix the normalization factor to be

$$\begin{aligned} \mathcal{N}_1^{klm} &= -i(-1)^{l+1} \delta_{m1} \sqrt{\frac{4\pi(2l+1)}{l(l+1)}} \frac{1}{2k\mathcal{I}_1(u \rightarrow \infty)}, \\ \mathcal{N}_2^{klm} &= (-1)^l \delta_{m1} \sqrt{\frac{4\pi(2l+1)}{l(l+1)}} \frac{1}{2k\mathcal{I}_2(u \rightarrow \infty)}. \end{aligned} \quad (\text{C2})$$

We proceed with this crude approximation, considering only the effect in the static limit $u \rightarrow \infty$ and time dependent effect in the energy density will come from the rest of the part of the solution. We follow the definition of the incident energy density discussed in the previous section,

$$\partial_u \mathcal{G}_{in} = \mathcal{T}^z{}_u = [\mathcal{T}_{uz} - \mathcal{T}_{uu}], \quad (\text{C3})$$

but we will transform this quantity to the spherical coordinate using, $\mathcal{T}'_{\mu\nu}(x') = (\partial x^\alpha / \partial x'^\mu) (\partial x^\beta / \partial x'^\nu) \mathcal{T}_{\alpha\beta}(x)$ So, after simplification,

$$\partial_u \mathcal{G} = \left\{ \frac{1}{2} g^{ss} (\partial_u A_s - \partial_s A_u) (\partial_r A_s^* - \partial_s A_r^*) + c.c. \right\} - g^{ss} (\partial_u A_s - \partial_s A_u) (\partial_u A_s^* - \partial_s A_u^*) \quad (\text{C4})$$

and as the incident plane wave is considered to be propagating along the z-direction we suitably choose, $\theta \rightarrow 0$, as per the requirement.

In the following discussion, we want to express the gauge invariant combinations taking only the ingoing part of (C1),

$$\begin{aligned} \partial_u A_s - \partial_s A_u &= \sum_{lm} [(\partial_r \chi_1^{lm} - \partial_u \chi_1^{lm}) \Psi_s^{lm}(\Omega) + \partial_u \chi_2^{lm} \Phi_s^{lm}(\Omega)] \\ &= i \sum_{lm} (-1)^{l+1} \delta_{m1} \sqrt{\frac{4\pi(2l+1)}{l(l+1)}} \left[\frac{i}{k} \frac{d}{du} \left(\frac{\mathcal{I}_2^{lm}(u)}{\mathcal{I}_2^{lm}(u \rightarrow \infty)} \right) \Phi_s^{lm} + \frac{\mathcal{I}_2^{lm}(u)}{\mathcal{I}_2^{lm}(u \rightarrow \infty)} \Phi_s^{lm} + \frac{i}{k} \frac{d}{du} \left(\frac{\mathcal{I}_1^{lm}(u)}{\mathcal{I}_1^{lm}(u \rightarrow \infty)} \right) \Psi_s^{lm} \right. \\ &\quad \left. + \frac{\mathcal{I}_1^{lm}(u)}{\mathcal{I}_1^{lm}(u \rightarrow \infty)} i \Psi_s^{lm} \right] \frac{e^{-ik(u+2r)}}{2} + \text{outgoing part} \end{aligned} \quad (\text{C5})$$

$$\begin{aligned} \partial_r A_s - \partial_s A_r &= \sum_{lm} [\partial_r \chi_1^{lm} \Psi_s + \partial_r \chi_2^{lm} \Phi_s] \\ &= 2i \sum_{lm} (-1)^{l+1} \delta_{m1} \sqrt{\frac{4\pi(2l+1)}{l(l+1)}} \left[\frac{\mathcal{I}_2^{lm}(u)}{\mathcal{I}_2^{lm}(u \rightarrow \infty)} \Phi_s^{lm}(\Omega) + \frac{\mathcal{I}_1^{lm}(u)}{\mathcal{I}_1^{lm}(u \rightarrow \infty)} i \Psi_s^{lm}(\Omega) \right] \frac{e^{-ik(u+2r)}}{2} + \text{outgoing part} \end{aligned}$$

where we have used the equations governing the gauge invariant variables in (u, r) coordinate for asymptotic Schwarzschild space-time (One may look at Appendix.D) as our aim to calculate the absorption cross section at $r \rightarrow \infty$. We express the above invariant combinations in Cartesian Coordinates in the following way :

$$\begin{aligned}
& \partial_u A_s - \partial_s A_u \\
&= \frac{\sum_{lm} (-1)^{l+1} \delta_{m1} \sqrt{\frac{4\pi(2l+1)}{l(l+1)}} \left[\frac{i}{k} \frac{d}{du} \left(\frac{\mathcal{I}_2^{lm}(u)}{\mathcal{I}_2^{lm}(u \rightarrow \infty)} \right) \Phi_s^{lm} + \frac{\mathcal{I}_2^{lm}(u)}{\mathcal{I}_2^{lm}(u \rightarrow \infty)} \Phi_s^{lm} + \frac{i}{k} \frac{d}{du} \left(\frac{\mathcal{I}_1^{lm}(u)}{\mathcal{I}_1^{lm}(u \rightarrow \infty)} \right) \Psi_s^{lm} + \frac{\mathcal{I}_1^{lm}(u)}{\mathcal{I}_1^{lm}(u \rightarrow \infty)} i \Psi_s^{lm} \right]}{\sum_{lm} (-1)^{l+1} \delta_{m1} \sqrt{\frac{4\pi(2l+1)}{l(l+1)}} [\Phi_s^{lm}(\Omega) + i \Psi_s^{lm}(\Omega)]} \times \\
& \times (-ik A'_s(u, \mathbf{r})) \\
&= \xi_{us}(k, l, u) (-ik A'_s(u, \mathbf{r})) \\
& \partial_r A_s - \partial_s A_r = \frac{\sum_{lm} (-1)^{l+1} \delta_{m1} \sqrt{\frac{4\pi(2l+1)}{l(l+1)}} \left[\frac{\mathcal{I}_2^{lm}(u)}{\mathcal{I}_2^{lm}(u \rightarrow \infty)} \Phi_s^{lm}(\Omega) + \frac{\mathcal{I}_1^{lm}(u)}{\mathcal{I}_1^{lm}(u \rightarrow \infty)} i \Psi_s^{lm}(\Omega) \right]}{\sum_{lm} (-1)^{l+1} \delta_{m1} \sqrt{\frac{4\pi(2l+1)}{l(l+1)}} [\Phi_s^{lm}(\Omega) + i \Psi_s^{lm}(\Omega)]} (-2ik A'_s(u, \mathbf{r})) \\
&= \xi_{rs}(k, l, u) (-2ik A'_s(u, \mathbf{r}))
\end{aligned} \tag{C6}$$

where, $\xi_{rs}(k, l, u)$, $\xi_{us}(k, l, u)$ has to be evaluated numerically, and $A'_s(u, \mathbf{r})$ is the spherical representation of the plane wave in flat space. Substituting the above combinations in the expression of incident energy density we arrive at,

$$\begin{aligned}
\partial_u \mathcal{G} &= \left\{ \frac{1}{2} g^{ss} (\partial_u A_s - \partial_s A_u) (\partial_r A_s^* - \partial_s A_r^*) + c.c. \right\} - g^{ss} (\partial_u A_s - \partial_s A_u) (\partial_u A_s^* - \partial_s A_u^*) \\
&= 2 \left\{ \frac{k^2}{2} g^{ss} \xi_{us}(k, l, u) \xi_{rs}^*(k, l, u) A'_s(u, \mathbf{r}) A'^*_s(u, \mathbf{r}) + c.c. \right\} - k^2 g^{ss} |\xi_{us}(k, l, u)|^2 A'_s(u, \mathbf{r}) A'^*_s(u, \mathbf{r})
\end{aligned} \tag{C7}$$

As a consistency check, one may look for the case of static black hole limit, which corresponds to $u \rightarrow \infty$. In this limit the components (C6) become

$$\begin{aligned}
\partial_u A_s - \partial_s A_u &= -ik A'_s(u, \mathbf{r}) \\
\partial_r A_s - \partial_s A_r &= -2ik A'_s(u, \mathbf{r})
\end{aligned} \tag{C8}$$

by substituting these combinations

$$\partial_u \mathcal{G} = 2k^2 \cos^2 \theta + 2k^2 - k^2 \cos^2 \theta - k^2 = 2k^2 \tag{C9}$$

and as the incident plane wave is considered to be propagating along the z-direction we suitably choose, $\theta \rightarrow 0$.

Appendix D: Gauge Field Equation in (u, r) Coordinate For Schwarzschild BH

In this section, we discuss the coordinate transformation from (t, \mathbf{r}) to $(u(=t-r^*), \mathbf{r})$ and derive the expressions for EM field components and their invariant combinations. Consider the general definition of coordinate transformation for rank-1 tensor, from $x^\mu(t, r) \rightarrow x'^\mu(u, r)$, given as [46],

$$\tilde{A}_\mu(x') = \frac{\partial x^\nu}{\partial x'^\mu} A_\nu(x) \tag{D1}$$

under which the components (5) of the EM wave transform as

$$\begin{aligned}
\tilde{A}_u(u, \mathbf{r}) &= \frac{\partial t}{\partial u} A_t(t, \mathbf{r}) = A_t(t, \mathbf{r}) = b^{lm}(t, r) Y_{lm}(\Omega) \\
\tilde{A}_r(u, \mathbf{r}) &= \frac{\partial t}{\partial r} A_t(t, \mathbf{r}) + \frac{\partial r}{\partial r} A_r(t, \mathbf{r}) = \frac{1}{f(r)} A_t(t, \mathbf{r}) + A_r(t, \mathbf{r}) = \left(h^{lm}(t, r) + \frac{b^{lm}(t, r)}{f(r)} \right) Y_{lm}(\Omega) \\
\tilde{A}_\theta(u, \mathbf{r}) &= A_\theta(t, \mathbf{r}) \\
\tilde{A}_\phi(u, \mathbf{r}) &= A_\phi(t, \mathbf{r})
\end{aligned} \tag{D2}$$

One can see that only one of the components changes due to the coordinate transformation, that is, $\tilde{h}^{lm}(u, r) = h^{lm}(u+r^*, r) + b^{lm}(u+r^*, r)/f(r)$. Utilizing this we rewrite the components of the propagating EM wave as,

$$\begin{aligned}
\tilde{A}_u(u, \mathbf{r}) &= b^{lm}(u, r) Y_{lm}(\Omega) \\
\tilde{A}_r(u, \mathbf{r}) &= \tilde{h}^{lm}(u, r) Y_{lm}(\Omega) \\
\tilde{A}_s(u, \mathbf{r}) &= k_{lm}(u, r) \Psi_s^{lm}(\Omega) + a_{lmk}(u, r) \Phi_s^{lm}(\Omega).
\end{aligned} \tag{D3}$$

From the equation of motion, $\nabla_\mu F^{\mu\nu} = 0$, one gets the following coupled equation of the EM field propagating in Schwarzschild space time,

$$\begin{aligned}\partial_r \tilde{\chi}_1^{lm} + \tilde{\chi}_3^{lm} &= 0 \\ \partial_u \tilde{\chi}_1^{lm} + f(r) \tilde{\chi}_3^{lm} - \tilde{\chi}_4^{lm} &= 0,\end{aligned}\tag{D4}$$

which can be further combined to obtain a decoupled equation of the following form

$$\partial_r(f(r)\partial_r \tilde{\chi}_1^{lm}) - 2\partial_u \partial_r \tilde{\chi}_1^{lm} - \frac{l(l+1)}{r^2} \tilde{\chi}_1^{lm} = 0.\tag{D5}$$

Also, the equation governing $\tilde{\chi}_2^{lm}$ turns out to be,

$$\partial_r(f(r)\partial_r \tilde{\chi}_2^{lm}) - 2\partial_u \partial_r \tilde{\chi}_2^{lm} - \frac{l(l+1)}{r^2} \tilde{\chi}_2^{lm} = 0\tag{D6}$$

where the expression for transformed invariant variables are $\tilde{\chi}_1^{lm}(u, r) = \frac{r^2}{l(l+1)}(\partial_u \tilde{h}^{lm}(u, r) - \partial_r b^{lm}(u, r))$ and $\tilde{\chi}_2^{lm}(u, r) = \tilde{a}^{lm}(u, r) = a^{lm}(u + r_*, r)$. Other invariant variables can be computed from the above constrained equation (D4).

-
- [1] B. P. Abbott *et al.* [LIGO Scientific and Virgo], Phys. Rev. Lett. **116**, no.6, 061102 (2016)
- [2] B. P. Abbott *et al.* [LIGO Scientific and Virgo], Phys. Rev. Lett. **116**, no.13, 131103 (2016)
- [3] B. P. Abbott *et al.* [LIGO Scientific and Virgo], Phys. Rev. D **93**, no.12, 122003 (2016)
- [4] B. P. Abbott *et al.* [LIGO Scientific and Virgo], Phys. Rev. Lett. **116**, no.24, 241102 (2016)
- [5] B. P. Abbott *et al.* [LIGO Scientific and Virgo], Phys. Rev. Lett. **116**, no.24, 241103 (2016)
- [6] B. P. Abbott *et al.* [LIGO Scientific and Virgo], Phys. Rev. Lett. **119**, no.14, 141101 (2017)
- [7] B. P. Abbott *et al.* [LIGO Scientific and Virgo], Phys. Rev. Lett. **119**, no.16, 161101 (2017)
- [8] R. Abbott *et al.* [LIGO Scientific and Virgo], Phys. Rev. D **102**, no.4, 043015 (2020)
- [9] B. P. Abbott *et al.* [LIGO Scientific and Virgo], Phys. Rev. Lett. **118**, no.12, 121101 (2017) [erratum: Phys. Rev. Lett. **119**, no.2, 029901 (2017)]
- [10] B. P. Abbott *et al.* [LIGO Scientific and Virgo], Astrophys. J. Lett. **892**, no.1, L3 (2020)
- [11] R. Abbott *et al.* [LIGO Scientific and Virgo], Astrophys. J. Lett. **896**, no.2, L44 (2020)
- [12] B. P. Abbott *et al.* [LIGO Scientific and Virgo], Astrophys. J. Lett. **851**, L35 (2017)
- [13] R. Abbott *et al.* [LIGO Scientific, Virgo and KAGRA], PoS **ICRC2023**, 1579 (2023)
- [14] R. Abbott *et al.* [KAGRA, VIRGO and LIGO Scientific], Astrophys. J. Suppl. **267**, no.2, 29 (2023)
- [15] R. Abbott *et al.* [KAGRA, VIRGO and LIGO Scientific], PTEP **2022**, no.6, 063F01 (2022)
- [16] J. Blackman, S. E. Field, M. A. Scheel, C. R. Galley, C. D. Ott, M. Boyle, L. E. Kidder, H. P. Pfeiffer and B. Szilágyi, Phys. Rev. D **96**, no.2, 024058 (2017)
- [17] J. Centrella, J. G. Baker, B. J. Kelly and J. R. van Meter, Rev. Mod. Phys. **82**, 3069 (2010)
- [18] M. Boyle, D. A. Brown, L. E. Kidder, A. H. Mroue, H. P. Pfeiffer, M. A. Scheel, G. B. Cook and S. A. Teukolsky, Phys. Rev. D **76**, 124038 (2007)
- [19] P. Ajith, S. Babak, Y. Chen, M. Hewitson, B. Krishnan, A. M. Sintes, J. T. Whelan, B. Bruegmann, P. Diener and N. Dorband, *et al.* Phys. Rev. D **77**, 104017 (2008) [erratum: Phys. Rev. D **79**, 129901 (2009)]
- [20] R. Karmakar and D. Maity, Phys. Rev. D **105**, no.10, 104045 (2022)
- [21] C. L. Benone and L. C. B. Crispino, Phys. Rev. D **99**, no.4, 044009 (2019)
- [22] A. Patel and A. Dasgupta, [arXiv:2108.01788 [gr-qc]].
- [23] Clarkson, C. A., Marklund, M., Betschart, G., & Dunsby, P. K. S. (2004). The Astrophysical Journal, 613(1), 492.
- [24] A. A. Starobinskii, Sov. Phys. JETP **64**, no.1, 48-57 (1973)
- [25] A. A. Starobinskii and S. M. Churilov, Sov. Phys. JETP **65**, no.1, 1-5 (1974)
- [26] L. C. B. Crispino, E. S. Oliveira, A. Higuchi and G. E. A. Matsas, Phys. Rev. D **75**, 104012 (2007)
- [27] L. C. S. Leite, S. Dolan and L. Crispino, C.B., Phys. Rev. D **98**, no.2, 024046 (2018)
- [28] L. C. S. Leite, S. R. Dolan and L. C. B. Crispino, Phys. Lett. B **774**, 130-134 (2017)
- [29] L. C. B. Crispino and E. S. Oliveira, Phys. Rev. D **78**, 024011 (2008)
- [30] V. Cardoso and R. Vicente, Phys. Rev. D **100**, no.8, 084001 (2019)
- [31] Y. Chen, X. Xue and V. Cardoso, [arXiv:2308.00741 [hep-ph]].
- [32] R. Roy and U. A. Yajnik, Phys. Lett. B **803**, 135284 (2020)
- [33] R. Roy, S. Vagnozzi and L. Visinelli, Phys. Rev. D **105**, no.8, 083002 (2022)
- [34] Y. Chen, J. Shu, X. Xue, Q. Yuan and Y. Zhao, Phys. Rev. Lett. **124**, no.6, 061102 (2020)
- [35] G. W. Yuan, Z. Q. Xia, C. Tang, Y. Zhao, Y. F. Cai, Y. Chen, J. Shu and Q. Yuan, JCAP **03**, 018 (2021)

- [36] F. J. Zerilli, Phys. Rev. D **2**, 2141 (1970). doi:10.1103/PhysRevD.2.2141
- [37] T. Regge and J. A. Wheeler, Phys. Rev. **108**, 1063 (1957). doi:10.1103/PhysRev.108.1063
- [38] L. A. Edelman and C. V. Vishveshwara, Phys. Rev. D **1**, 3514 (1970). doi:10.1103/PhysRevD.1.3514
- [39] F. J. Zerilli, Phys. Rev. Lett. **24**, 737-738 (1970) doi:10.1103/PhysRevLett.24.737
- [40] S. Chandrasekhar and S. L. Detweiler, Proc. Roy. Soc. Lond. A **344**, 441 (1975).
- [41] S. Chandrasekhar Proc. Roy. Soc. Lond. A **343**, 289-298 (1975).
- [42] R. Brito, V. Cardoso and P. Pani, Physics, Lect. Notes Phys. **906**, pp.1-237 (2015) 2020, [arXiv:1501.06570 [gr-qc]].
- [43] R G Barrera et al 1985 Eur. J. Phys. 6 287
- [44] J. D. Jackson, Wiley, 1998, ISBN 978-0-471-30932-1
- [45] W. G. Unruh, Phys. Rev. D **14**, 3251-3259 (1976)
- [46] T. Padmanabhan, Cambridge University Press, 2014, ISBN 978-7-301-22787-9
- [47] L. Rezzolla, ICTP Lect. Notes Ser. **14**, 255-316 (2003) [arXiv:gr-qc/0302025 [gr-qc]].
- [48] C. Molina, P. Pani, V. Cardoso and L. Gualtieri, Phys. Rev. D **81**, 124021 (2010)
- [49] D. C. Dai and D. Stojkovic, Phys. Lett. B **843**, 138056 (2023)
- [50] M. P. van Haarlem, M. W. Wise, A. W. Gunst, G. Heald, J. P. McKean, J. W. T. Hessels, A. G. de Bruyn, R. Nijboer, J. Swinbank and R. Fallows, *et al.* Astron. Astrophys. **556**, A2 (2013)
- [51] A. Corstanje, S. Buitink, J. E. Enriquez, H. Falcke, J. R. Hörandel, M. Krause, A. Nelles, J. P. Rachen, P. Schellart and O. Scholten, *et al.* Astron. Astrophys. **590**, A41 (2016)
- [52] S. Chandrasekhar, The maximum mass of ideal white dwarfs, *Astrophys. J.* 74, 81 (1931).
- [53] S. W. Hawking and W. Israel, "THREE HUNDRED YEARS OF GRAVITATION,"
- [54] M. Riajul Haque, E. Kpatcha, D. Maity and Y. Mambrini, Phys. Rev. D **108**, no.6, 063523 (2023)
- [55] I. Musco, Phys. Rev. D **100**, no.12, 123524 (2019)
- [56] M. Calzà, J. G. Rosa and F. Serrano, [arXiv:2306.09430 [hep-ph]].
- [57] N. P. Branco, R. Z. Ferreira and J. G. Rosa, JCAP **04**, 003 (2023)
- [58] J. G. Rosa and T. W. Kephart, Phys. Rev. Lett. **120**, no.23, 231102 (2018)
- [59] B. Carr, K. Dimopoulos, C. Owen and T. Tenkanen, Phys. Rev. D **97**, no.12, 123535 (2018)
- [60] B. Carr, K. Kohri, Y. Sendouda and J. Yokoyama, Rept. Prog. Phys. **84**, no.11, 116902 (2021)
- [61] A. Escrivà, F. Kuhnel and Y. Tada, [arXiv:2211.05767 [astro-ph.CO]].
- [62] M. Sasaki, T. Suyama, T. Tanaka and S. Yokoyama, *Class. Quant. Grav.* **35**, no.6, 063001 (2018)
- [63] B. Carr, S. Clesse, J. Garcia-Bellido, M. Hawkins and F. Kuhnel, [arXiv:2306.03903 [astro-ph.CO]].
- [64] A. Kashlinsky, Y. Ali-Haimoud, S. Clesse, J. Garcia-Bellido, L. Wyrzykowski, A. Achúcarro, L. Amendola, J. Annis, A. Arbey and R. G. Arendt, *et al.* [arXiv:1903.04424 [astro-ph.CO]].
- [65] D. N. Page, Phys. Rev. D **13**, 198-206 (1976)
- [66] S. W. Hawking, *Commun. Math. Phys.* **43**, 199-220 (1975)
- [67] I. Baldes, Q. Decant, D. C. Hooper and L. Lopez-Honorez, JCAP **08**, 045 (2020)
- [68] Giant Metrewave Radio Telescope, NCRA-TIFR
- [69] Gupta, Y., Ajithkumar, B., Kale, H.S., Nayak, S., Sabhapathy, S., Sureshkumar, S., *et al.*: 2017, *Current Science* **113**, 707.
- [70] H. T. Intema, P. Jagannathan, K. P. Mooley and D. A. Frail, *Astron. Astrophys.* **598**, A78 (2017)
- [71] A. Weltman, P. Bull, S. Camera, K. Kelley, H. Padmanabhan, J. Pritchard, A. Raccanelli, S. Riemer-Sørensen, L. Shao and S. Andrianomena, *et al.* *Publ. Astron. Soc. Austral.* **37**, e002 (2020)
- [72] National Radio Astronomy Observatory
- [73] S. Sanidas, S. Cooper, C. G. Bassa, J. W. T. Hessels, V. I. Kondratiev, D. Michilli, B. W. Stappers, C. M. Tan, J. van Leeuwen and L. Cerrigone, *et al.* *Astron. Astrophys.* **626**, A104 (2019)
- [74] D. Michilli, J. W. T. Hessels, R. J. Lyon, C. M. Tan, C. Bassa, S. Cooper, V. I. Kondratiev, S. Sanidas, B. W. Stappers and J. van Leeuwen, *Mon. Not. Roy. Astron. Soc.* **480**, no.3, 3457-3467 (2018)
- [75] D. Michilli, C. Bassa, S. Cooper, J. W. T. Hessels, V. I. Kondratiev, S. Sanidas, B. W. Stappers, C. M. Tan, J. van Leeuwen and I. Cognard, *et al.* *Mon. Not. Roy. Astron. Soc.* **491**, no.1, 725-739 (2020)
- [76] C. M. Tan, C. G. Bassa, S. Cooper, J. W. T. Hessels, V. I. Kondratiev, D. Michilli, S. Sanidas, B. W. Stappers, J. van Leeuwen and J. Y. Donner, *et al.* *Mon. Not. Roy. Astron. Soc.* **492**, no.4, 5878-5896 (2020)
- [77] R. Vicente, V. Cardoso and J. C. Lopes, Phys. Rev. D **97**, no.8, 084032 (2018)